Thermo-physical properties prediction of carbon-based magnetic nanofluids based on artificial neural network

Lei Shi[a,b], Shuai Zhang[b], Adeel Arshad[d], Yanwei Hu[a], Yurong He[a]*, Yuying Yan[b,c]

a School of Energy Science and Engineering, Harbin Institute of Technology, Harbin 150001 China

b Fluids & Thermal Engineering Research Group, Faculty of Engineering, University of Nottingham, NG7 2RD, UK

c Research Centre for Fluids and Thermal Engineering, University of Nottingham Ningbo China, Ningbo 315100, China

*Corresponding author. E-mail address: rong@hit.edu.cn

Abstract: Nanostructured magnetic suspensions have superior thermophysical properties, which have attracted widespread attention owing to their industrial applications for heat transfer enhancement and thermal management. However, experimental measurements of the thermophysical properties of magnetic-based nanofluids, especially under an external magnetic field, are significantly complicated, expensive, and time consuming. Currently, the method of predicting and summarizing material properties through machine learning has accelerated the development of materials and practical industrial applications. This study aims to predict the thermophysical properties of magnetic nanofluids by establishing an artificial neural network (ANN) using experimental data on viscosity, thermal conductivity, and specific heat. The results based on the ANN model agree with the experimental results according to the different evaluation criteria. Different previous theoretical thermophysical models are reviewed, and the ANN model is proven to be more accurate by comparing the values of the ANN model and previous thermophysical models, which can also provide a theoretical basis for explaining the heat transfer of magnetic nanofluids. In the present study, a neural network model was developed for predicting the thermophysical properties of magnetic nanofluids and using material informatics to study functional materials.

Keywords: Heat transfer; magnetic nanofluid; thermo-physical property; artificial neural network

Introduction

Fluid thermophysical properties are the key to estimating heat transfer performance and efficiency, which are almost ubiquitous in industrial fields [1-6]. Nanoparticles dispersed in base fluids are collectively known as nanofluids, and their potential applications in electron cooling and heat transfer have been investigated in recent years [3,4]. Depending on the types of particles received, nanofluids can be divided into metal nanofluids (Au, Ag, Cu, Ni, etc.), metal-oxide nanofluids (e.g., ZnO, TiO_2, Fe_3O_4, Al_2O_3), and nonmetallic nanofluids (e.g., carbon nanotube (CNT), graphene) [5,6]. Based on a report by Choi in 1995 [7,8], the nanofluid became popular as a coolant or thermal transport medium to obtain superior heat exchange efficiency when compared to the traditional working mediums in energy conversion systems [9,10]. According to the type of base fluid received, nanofluids included not only water-based nanofluids, but also oil-, ether-, and ester-based nanofluids [11,12]. Various experimental and numerical studies have focused on the heat transfer of nanofluids and their applications [4,13]. These studies have also shown that the superior thermal characteristics of nanofluids can be influenced by the thermophysical characteristics of the base liquid and nanoparticles [5,14].

Among the various nanofluids, magnetic nanofluids, which consist of a base fluid and superparamagnetic nanoparticles, have potential extensive applications in microfluidic chips, magnetofluid seals, and magnetic particle tracers because of their magnetic and fluid properties [15-19]. Magnetic nanofluids, such as Fe, Co, Ni, and their oxides, are usually prepared using magnetic materials with different morphologies and sizes [20-24]. Comparing to most nanofluids such as ZnO, TiO_2, and Al_2O_3 nanofluids, the cost of magnetic nanofluids is generally low because of their low-priced raw materials and convenient preparation process [25,26]. The primary objective of using nanofluids for heat transfer applications is to enhance the thermal conductivity, which is achieved by adding nanoparticles [16,27]. Although the heat conduction performance of magnetic nanofluids has been reported [28], the mechanisms for explaining the measured experimental data under applied magnetism are still ambiguous [7,29]. In heat transfer applications, the development of controllable thermophysical properties of nanofluids is a new research hotspot [30,31]. However, magnetic nanofluids that are suitable for different heat transfer applications require conditions such as high specific heat and high conductivity [32,33]. Hence, the primary research topics include the control of nanofluid saturation susceptibility, free surface characteristics, and magnetorheological characteristics of magnetic nanofluids under applied magnetism [34-36]. With the growing demand for magnetic nanofluids with higher thermal conductivity, carbon-based magnetic nanofluids [36], which consist of base fluid and carbon-based magnetic nanoparticles (**Fig. 1**), have become increasingly attractive because of their superior thermal conduction and magnetism [37-41]. The use of carbon-based magnetic nanofluids as the working medium is of great significance [42,43]. Particularly, the possibility of inducing and controlling heat transfer processes and fluid flow through an external magnetic field has enhanced the energy conversion of magnetrons in heat transfer systems [44-49].

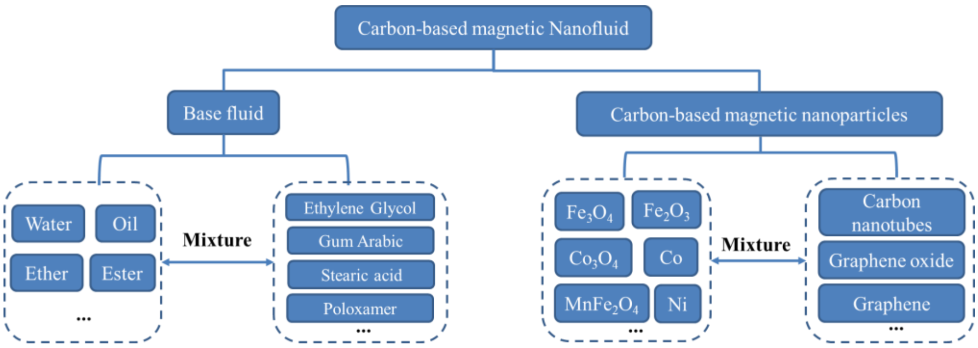

Fig. 1 Components of carbon-based magnetic nanofluids

The enhancement of heat transfer using carbon-based magnetic nanofluids under external magnetism is defined as a compound thermal management technique that enhances the heat transfer process [50-53]. As an important branch of fluid mechanics, the coupling problem between magnetohydrodynamics and heat transfer has not yet been solved, although it has been investigated [16,17]. In terms of experiments, owing to the different research contents, the thermal properties of the same nanofluid, such as specific heat, viscosity, thermal conductivity, and other systems, are rarely tested in the same work [54]. For this reason, it is difficult to evaluate the thermal characteristics of nanofluids based on a single thermophysical property [55]. However, because the magnetic particles in a magnetic liquid under a magnetic field, which are under the action of thermophysical properties, especially viscosity and thermal conductivity, will exhibit corresponding changes [56,57], this type of dynamic distribution of magnetic particles under the thermophysical experimental measurement of magnetic liquids is significantly difficult [58,59]; consequently, so far, only a few reports have been published on the related theory of thermophysical properties under the action of magnetism [60,61]. The factors affecting the thermophysical properties of nanofluids have not been completely clarified; however, these factors are certainly affected by the base fluids, nanoparticles, and external field (**Fig. 2**) [55-62]. Many of the influencing factors are not simply independent but have a complex coupling relationship [38,63]. For example, the Brownian motion of nanoparticles can increase the chance of collision between nanoparticles and affect the agglomeration of solids in the suspension; moreover, this motion is related to the size of nanoparticles, which can further affect the Brownian motion of nanoparticles [39,64]. Although several theoretical investigations and experimental studies have investigated the thermal and physical characteristics of different suspensions, related theories based on the characteristics of solid particles and liquids are still not appropriate for forecasting the thermal characteristics of nanofluids under an external field [65-68]. Therefore, it is essential to develop a new modeling method for nanofluids to better describe the impact of several factors on the thermophysical characteristics qualitatively and characterize the strengthening characteristics of the thermophysical properties of nanofluids [40,69].

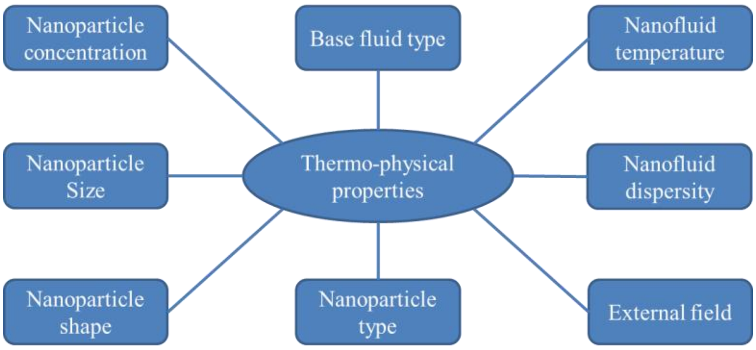

Fig. 2 Analysis of factors that can affect the thermo-physical of carbon-based magnetic nanofluids

Materials informatics is an emerging field that exploits the achievement of information technology to advance the exploration of the utilization, selection, development, and discovery of materials [31-33]. Comparing to experimental measurement, materials informatics only needs the cost of the calculation, which can replace the expense of experimental equipment and materials to a certain extent [70,71]. In the widely accepted scheme of determining structure–property relationships, the nonlinear and coupling problems are still a big challenge while directly modeling these relationships. Hence, material informatics provides an alternative way to predict them without too much concern for domain-specific assumptions and models [35]. Machine learning is a problem-solving approach based on a probability distribution model and statistical analysis rather than a domain-specific model. This significantly enlarges the application scope of machine learning approaches [66,73]. Generally, machine learning can be roughly divided into three categories: supervised learning, unsupervised learning, and reinforcement learning [22]. The work presented in this paper is under the category of supervised learning. Since the breakthrough of deep neural networks in the computer vision community in 2012, industry and academia have turned their attention to applying artificial intelligence methods to their specific domains [22,71]. A series of successes in other totally different applications prove the significant generality and flexibility of neural networks. There are several variants of artificial neural networks (ANNs), such as convolutional neural networks, recurrent neural networks, and long short-term memory networks [22,66]. Each of these networks is adapted to specific domains and with its own built-in inductive bias. The essential structure of an ANN contains at least three layers, including one input layer, one output layer, and several hidden layers. The neural network can be deployed during the training and testing stages [30]. Initially, a weight vector is randomly assigned. In the process of information transmission, the learning samples are input into the input layer. The output vector is obtained based on the initial weight vector. Then, the network calculates the error between the output and target output vectors. Through error backpropagation, the network corrects the weight based on the gradient descent method to obtain an optimal solution [22,24]. Weights are updated automatically while minimizing the error function on the training set until the error no longer decreases.

The error in the testing set is an identifier of underfitting or overfitting and can be used as a reference to manually tune hyperparameters such as the learning rate or regularization coefficient [68]. On this basis, the thermophysical modeling theory of nanofluids is further improved [24,72]. Utilizing ANNs for thermophysical modeling is highly advantageous [24,73]. As a type of typical "black box" modeling technology, the ANN can effectively replicate the self-learning ability of natural neurons, i.e., the faculty of "memory"; moreover, setting up of the related process parameters is not required to achieve an accurately function model [70-74]; in addition, the directed graph topology can be used to approach nonlinear relationships with a degree of accuracy; further, ANNs also have the strong ability of self-organization and are adaptive [42-44]. With a high-dimensional parameter space, the ANN is sufficiently flexible to represent the coupling and uncertain relationship of complex nanofluid thermophysical properties. In addition, the exponential development of infrastructure related to ANN has made it more accessible, with an unprecedented utilization in the intelligent industry [66].

In this paper, an artificial intelligence approach for forecasting the thermophysical properties (viscosity, specific heat, and thermal conductivity) of carbon-based magnetic nanofluids is proposed. First, carbon-based magnetic nanofluids were prepared, and the thermophysical properties with different magnetic volume fractions in nanomaterials (φ_m), organic ethylene glycol (EG) mass fractions in the base fluid (φ_e), nanomaterial volume fractions in the nanofluid (φ_n), temperatures (T), and magnetic field strengths (M) were measured. Then, an optimal ANN was designed using experimental data. "Root mean square error" (RMSE), "mean absolute percentage error" (MAPE), "coefficient of determination" (R^2), and "mean square error" (MSE) were determined to evaluate this proposed model. Finally, different previous models were reviewed, and their performances were compared with those of the ANN models to predict the thermophysical properties of the carbon-based magnetic nanofluids. The purpose of this work is to evaluate and forecast the thermophysical properties of carbon-based magnetic nanofluids by considering multiple factors using machine learning and statistical analysis.

2. Experimental setup and research methodology

2.1. Artificial neural network (ANN) and simulation

The procedure in material informatics for determining the thermophysical properties of carbon-based magnetic nanofluids is shown in **Fig. 3**. The structure of the ANN shows the connection between the neural layers and the neurons, and the model for predicting the thermophysical properties is used to build a bridge from the small amount of experimental and simulated data to practical application based on thermal exchange and flow of nanofluids. ANNs take inspiration from the human brain, which is a densely connected and packed network from the perspective of neurologists [62]. However, essentially and more mathematically, the ANN is a parametric functional approximation with several parameters to be fitted with the data [63]. The training of the ANN is cast into an optimization problem of the cost function in the ANN weight-parameter space. Given sufficient observations of dependable and undependable variables, the ANN is able to extract the underlying functional relationships and abstract features inside the data. The pipeline of the general machine learning approach in material informatics consists of the following three parts. (1) Data collection: Data are typically generated by simulations or experiments conducted by material analysis. (2) Data representation: Raw data in the real world are usually dirty and the unreasonable outliers must be removed. Rescaling of the data scope and removing unrelated features can improve the robustness and convergence of algorithms. (3) Data mining: It involves the exploration of the underlying relationship between structural features and desired properties [64]. During the training process, weights are updated using an efficient and popular stochastic gradient descent (SGD) method. Hyperparameters and the regularization method can be chosen appropriately based on the model performance on the test set, or alternatively, by cross validation. The tangent–sigmoid function is chosen as the transfer function in the hidden layers, while the output layer is without a transfer function. Furthermore, the training algorithm adopts backpropagation, which is the Adam algorithm version of the SGD. Five input dimensions were considered in this study, including the magnetic volume fraction in nanomaterials (φ_{m}), organic mass fraction in base fluid (φ_{e}), nanomaterial volume fraction in the nanofluid (φ_{n}), temperature (T), and magnetic field strength (M). The three output parameters were the specific heat capacity (C_{p}), viscosity (μ), and thermal conductivity (k).

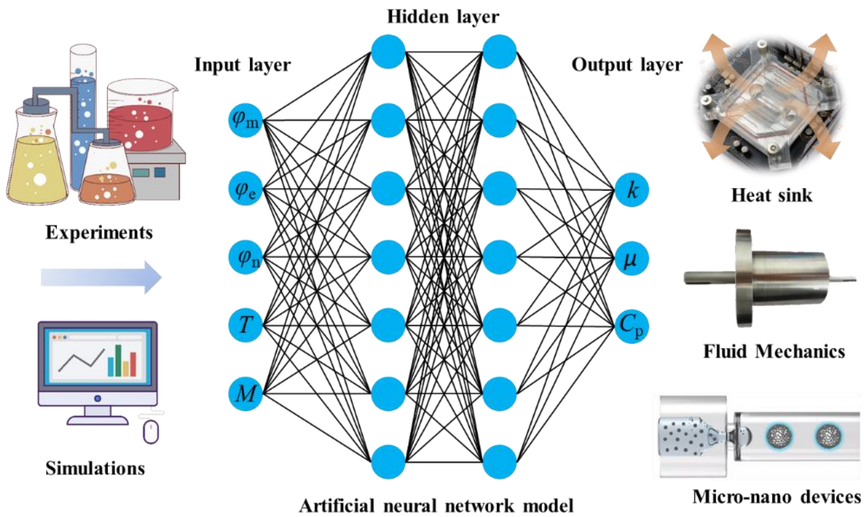

Fig. 3 Schematic diagram of artificial neural network structure predicting thermo-physical properties

ANN techniques in machine learning commonly use a multilayer perceptron (MLP) network, which is one of the most valued methods of monitored networks. Inspired by the biological neural network (**Fig. 4a**), the function of the ANN model is to build a regression relationship between the thermophysical properties and various operating conditions using carbon-based magnetic nanofluids. The network architecture is constructed without recurrent or lateral connections, falling into the large category of feedforward networks [69]. The information in our dataset flows into the network from the input layers. The input data are forward propagated by each hidden layer and extracted into more manipulable features in the next hidden layer. The transfer function in each hidden layer is employed to change the input-output relationship from linear to nonlinear. If not, the MLP is equivalent to a trivial one-layer perceptron. Finally, the three thermophysical properties are obtained from the output layer [70]. All the weights between layers can be updated efficiently by a backpropagation algorithm to minimize the training error. Data processing within one neuron is shown in **Fig. 4b**. By assuming n inputs that are applied to the network, and an activation function f, the transitive output y of one neuron is defined as the weighted sum of its inputs. w_i is the connection weight of the neuron and b is the bias. The process can be formulated as [71]:

$$y = f(\sum_{i=1}^{n} w_i x_i + b) \tag{1}$$

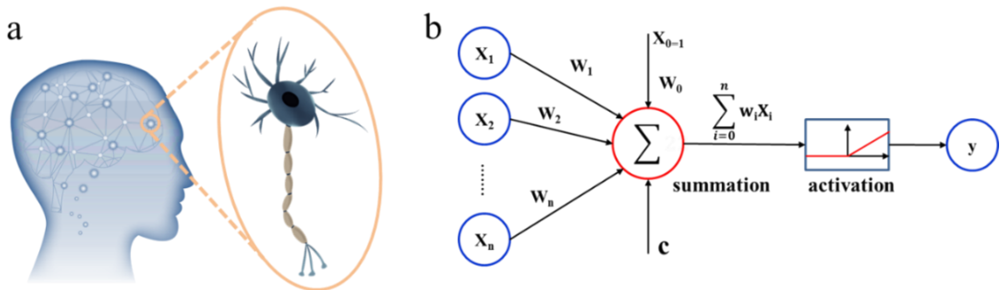

Fig. 4 (a) Schematic diagram of the biological neural network (b) The flow chart of data processing within a neuron [71]

2.2. Experimental preparation and characterization of magnetic nanofluids

Material preparation: Iron (II) chloride tetrahydrate, EG, CNTs, iron (III) chloride hexahydrate, Co_3O_4 nanoparticles, Ni nanoparticles, and ammonia solution were purchased from Aladdin Reagent (Shanghai, China). Deionized water (DW) that was purified in a laboratory-based ultrapure water system (arium mini plus; Sartorius, Göttingen, Germany) was used in all experiments. All reagents were used without further treatment because they were of analytical grade. The preparation and characterization of carbon-based magnetic nanofluids have been reported as follows. Two different iron (II) chloride tetrahydrate compounds were mixed with DW. Then, the ammonia solution was added and maintained at 80 °C. Subsequently, the dark Fe_3O_4 was combined with CNTs in different ratios (1:1, 2:1, 3:1, and 4:1) in DW under ultrasonic vibration. After drying, the Fe_3O_4/CNT composites were added to EG/DW solution, which was prepared in different ratios (1:1, 2:1, 3:1, and 4:1) in advance. The thermal conductivity was measured using a conductometer (TC-3000L, Xiatech Electronic Technology, China), as shown in **Fig. 5a**. As Co_3O_4, Ni, and Fe_3O_4 nanofluids showed nearly indiscriminate thermal conductivity when using the same volume fraction, Co_3O_4, Ni, and Fe_3O_4 nanoparticles can be regarded as unified magnetic nanoparticles when their nanofluids only serve as the working media for heat transfer. With an increase in the EG mass fraction (**Fig. 5b**) in the base fluid from 1:1 to 4:1, the thermal conductivity decreased, because EG weakens the thermal conduction between the DW and the nanoparticles. Conversely, when the magnetic nanoparticle mass fraction (**Fig. 5c**) in nanofluids was increased from 1:1 to 4:1, the thermal conductivity increased with an increase in the volume fraction, as depicted in **Fig. 5d**.

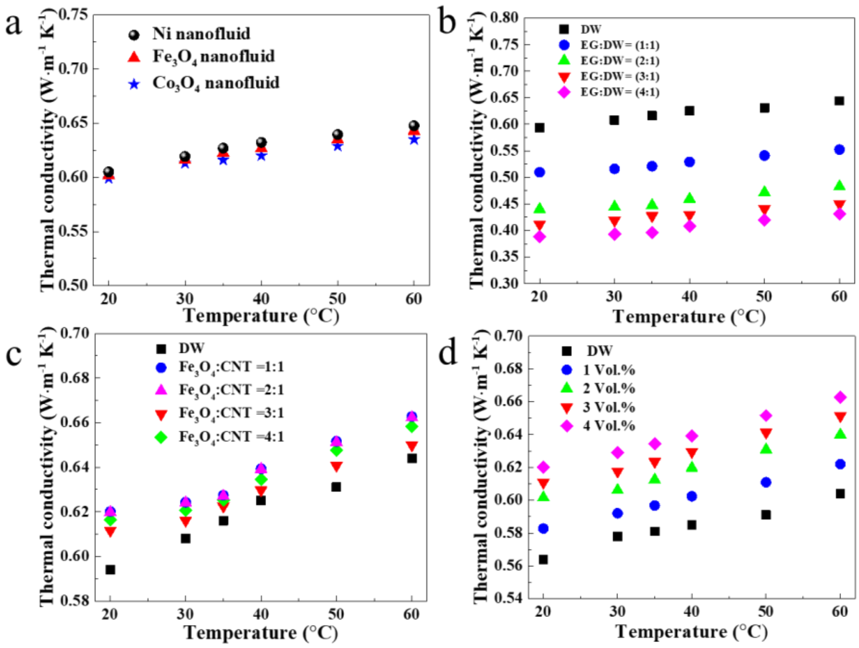

Fig. 5 Experimental thermal conductivity data of magnetic nanofluids: (a) Different nanoparticles (Ni, Fe_3O_4, Co_3O_4); (b) Different ethylene glycol (EG) mass fractions in base fluid; (c) Different magnetic volume fractions in nanomaterials; (d) Different magnetic volume fractions in nanomaterial

The rheological properties of the carbon-based magnetic nanofluids were measured using a super rheometer (Kinexus PRO, Malvern, US). From **Fig. 6a**, it can also be noted that Co_3O_4, Ni, and Fe_3O_4 can be regarded as unified magnetic nanoparticles because of their undifferentiated viscosity. With the increase in EG mass fraction (**Fig. 6b**) in the base fluid from 1:1 to 4:1, the viscosity of carbon-based magnetic nanofluids increased because EG has a higher viscosity when compared to DW. Conversely, when increasing the Fe_3O_4 mass fraction (**Fig. 6c**) in carbon-based magnetic nanofluids from 1:1 to 4:1, the viscosity of carbon-based magnetic nanofluids increased because the density of carbon-based magnetic nanofluids increases when the volume fraction is constant. The viscosity of carbon-based magnetic nanofluids increased with increasing volume concentration, as shown in **Fig. 6d**.

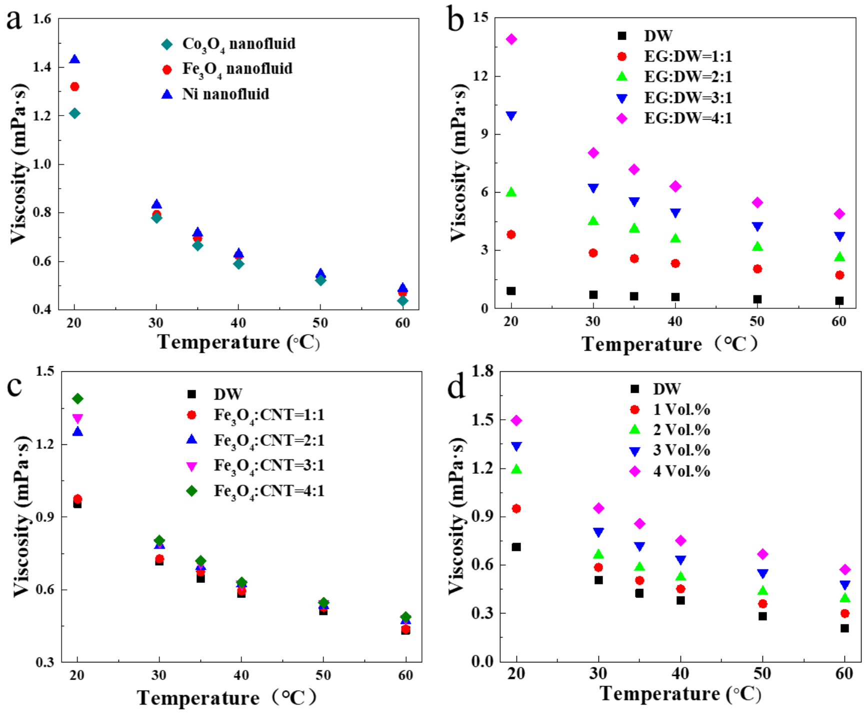

Fig. 6 Experimental viscosity data of magnetic nanofluids: (a) Different nanoparticles (Ni, Fe_3O_4, Co_3O_4); (b) Different EG mass fractions in base fluid; (c) Different magnetic volume fractions in nanomaterials; (d) Different magnetic volume fractions in nanomaterial

The specific thermal capacities of the carbon-based magnetic nanofluids were measured using a differential scanning calorimeter (204 FI, Netzsch, Germany) based on the sapphire method. Similar to viscosity and thermal conductivity, Co_3O_4, Ni, and Fe_3O_4 nanoparticles can be regarded as unified magnetic nanoparticles while measuring the specific heat capacity (**Fig. 7a**). With the increase in EG mass fraction (**Fig. 7b**) in the base fluid from 1:1 to 4:1, the specific heat of carbon-based magnetic nanofluids decreased because the EG weakens the specific heat of the base liquid when compared to DW. In contrast to the other parameters, when increasing the Fe_3O_4 mass fraction (**Fig. 7c**) in carbon-based magnetic nanofluids from 1:1 to 4:1, the specific heat of the carbon-based magnetic nanofluids decreased. Meanwhile, the specific heat of carbon-based magnetic nanofluids with different volume concentrations was investigated, as shown in **Fig. 7d**. The specific heat of the carbon-based magnetic nanofluids decreased with an increase in the volume fraction from 0 to 4 vol. %.

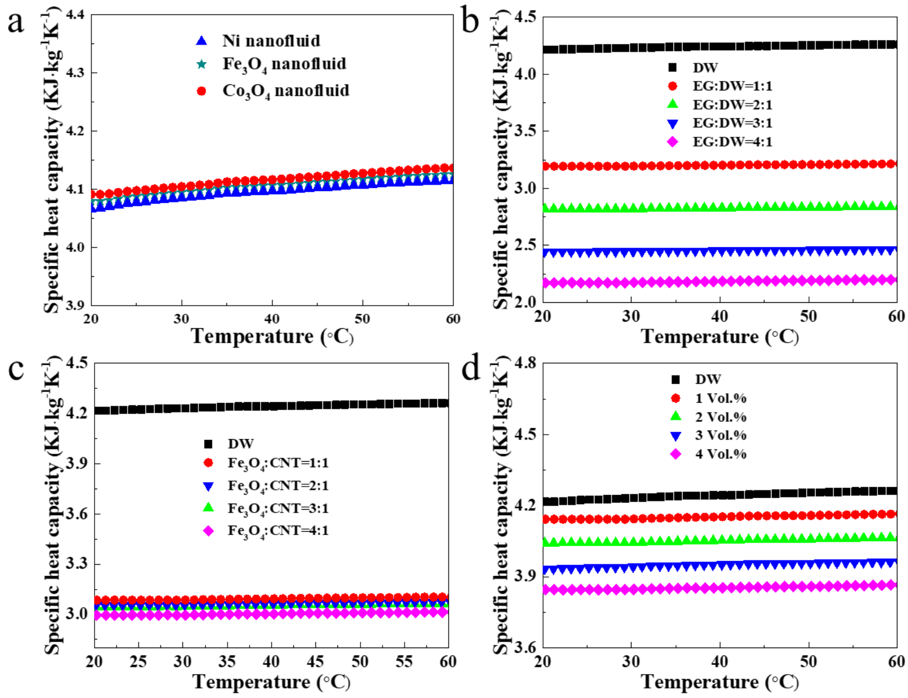

Fig. 7 Experimental specific heat capacity data of magnetic nanofluids: (a) Different nanoparticles (Ni, Fe_3O_4, Co_3O_4); (b) Different EG mass fractions in base fluid; (c) Different magnetic volume fractions in nanomaterials; (d) Different magnetic volume fractions in nanomaterial

2.3. Data acquisition of thermophysical properties of materials

For an effective data-driven prediction method, obtaining a sufficient amount of sample data is the key to accurate neural network prediction. The thermophysical properties of carbon-based magnetic nanofluids were predicted and analyzed by the neural network by selecting the experimental data of thermophysical properties published in existing literature and the measured data from previous experiments, which are listed in **Table 1** [45-69]; thus, 713 sets of published experimental data were employed as samples to be input to the model. The datasets were randomly divided into test, validation, and training data. The training dataset contained 70% of the total data and was used to adjust the weights of the network. The validation dataset, accounting for 15% of the total database, was utilized to minimize overfitting and affected the tuning of the weights. Finally, the remaining 15% of the collected data were employed to test the samples. To verify the effect of the above prognostic framework, sufficient sample data on the thermophysical properties of magnetic nanofluids were used to train and test the ANN model. The hardware and software configurations used in this work are as follows: Intel(R) Core(TM) i7-8700 CPU, Programming Language: Python 3.6, Pytorch 1.0.0.

Table 1 Experimental thermo-physical properties data of previous works used in neural network prediction

Date	Authors	Nanoparticles	Base fluids	Thermo-physical properties
2005	Li et al. [45]	Fe_3O_4	H_2O	thermal conductivity, viscosity
2009	Phuoc et al. [46]	Fe_2O_3	H_2O	thermal conductivity, viscosity
2010	Abareshi et al. [47]	Fe_3O_4	H_2O	thermal conductivity
2010	Wright et al. [48]	Ni/CNT	H_2O	thermal conductivity
2012	Sundar et al. [49]	Fe_3O_4	EG/DW	viscosity
2012	Colla et al. [50]	Fe_2O_3	H_2O	thermal conductivity
2013	Ghofrani et al. [51]	Fe_3O_4	H_2O	viscosity
2013	Sundar et al. [52]	Fe_3O_4	H_2O	thermal conductivity, viscosity
2014	Yu et al. [53]	Fe_3O_4	kerosene	thermal conductivity
2014	Sundar et al. [54]	MWCNT-Fe_3O_4	H_2O	thermal conductivity, viscosity
2014	Sundar et al. [55]	Ni	H_2O	thermal conductivity, viscosity, specific heat capacity
2015	Esfe et al. [56]	Fe	H_2O	thermal conductivity, viscosity
2015	Mariano et al. [57]	Co_3O_4	EG/DW	thermal conductivity, viscosity
2015	Karimi et al. [58]	Ni	H_2O	thermal conductivity
2016	Afrand et al. [59]	Fe_3O_4	EG/DW	viscosity
2016	Harandi et al. [60]	MWCNTs-Fe_3O_4	EG	thermal conductivity
2016	Shahsavar et al. [61]	CNT/Fe_3O_4	H_2O	thermal conductivity, viscosity, specific heat capacity
2016	Wang et al. [62]	Fe_3O_4	H_2O	viscosity
2016	Kumar et al. [63]	Fe_2O_3	EG/DW	thermal conductivity
2016	Nurdin et al. [64]	Fe_2O_3	H_2O	thermal conductivity, viscosity
2017	Esfe et al. [65]	Co_3O_4	EG/DW	thermal conductivity, viscosity
2017	Amani et al. [66]	$MnFe_2O_4$	H_2O	thermal conductivity, viscosity
2018	Vinod et al. [67]	Fe_3O_4	H_2O	thermal conductivity, viscosity
2018	Shi et al. [68]	Fe_3O_4/CNT	H_2O	thermal conductivity, viscosity, specific heat capacity
2019	Fu et al. [69]	Fe_3O_4	EG/DW	thermal conductivity, viscosity, specific heat capacity
2019	In this work	Fe_3O_4/CNT	EG/DW	thermal conductivity, viscosity, specific heat capacity

2.4. Prediction model evaluation criteria

To assess the accuracy of the prediction results from the ANN model for correlation, the standardized coefficient was implemented to determine the influence of each specialty variable on the value of the dependent variable; moreover, deviation analysis of the thermophysical property ratio (*TPR*) can be calculated as follows:

$$SCD = \frac{TPR_{\mathrm{E}} - TPR_{\mathrm{p}}}{TPR_{\mathrm{E}}} \tag{2}$$

where SCD is the standardized coefficient of deviation and TPR_E and TPR_P indicate the predicted values and experimental data of the TPR, respectively. To evaluate the predictive performance of the ANN, the testing data that were not used during the training process were analyzed. We analyzed unused test samples during network training to evaluate the predictive performance of the neural networks. Different criteria were used to evaluate the quality and accuracy of the predictive network. Subsequently, the Marquardt–Levenberg algorithm [70] was incorporated into the curve fitting to obtain a stable value for the correlation coefficient. The algorithm examined the parameter with the minimum sum of the squared error between the experimental thermophysical property data and the prediction result of the standardized magnetic nanofluid [71,72]. The sum of the squared error was calculated using the following equation.

$$S = \sum_{\mathrm{i}=1}^{n} (TPR_{\mathrm{E}} - TPR_{\mathrm{p}})^2 \tag{3}$$

R^2 reflects the difference between the predicted value and the experimental result and is used to assess the validity of the results predicted by the ANN. The calculation is as shown in following equation [71].

$$\mathrm{R}^2 = 1 - \frac{\sum_{\mathrm{i}=1}^{n} (TPR_{\mathrm{E}} - TPR_{\mathrm{p}})^2}{\sum_{\mathrm{i}=1}^{n} (TPR_{\mathrm{E}} - \overline{TPR_{\mathrm{E}}})^2} \tag{4}$$

However, R^2 is not sufficient to judge whether the obtained results are valid in certain cases. Hence, other parameters such as the MSE, RMSE, and MAPE are determined to verify the predicted results, where *n* is the number of data in the test set [72].

$$\mathrm{MAPE} = \frac{100\%}{n} \sum_{\mathrm{i}=1}^{n} \left| \frac{TPR_{\mathrm{E}} - TPR_{\mathrm{p}}}{TPR_{\mathrm{E}}} \right| \tag{5}$$

A MAPE of 0% indicates a perfect model, and a MAPE greater than 100% indicates an inferior model.

$$\mathrm{RMSE}=\left[\frac{1}{n}\sum_{\mathrm{i}=1}^{n}(TPR_{\mathrm{E}}-TPR_{\mathrm{p}})\right]^{0.5} \tag{6}$$

RMSE measures the deviation between the observed and true values. It is often used as a standard for measuring the prediction results of machine learning models.

$$\mathrm{MSE}=\frac{1}{n}\sum_{\mathrm{i}=1}^{n}(TPR_{\mathrm{E}}-TPR_{\mathrm{p}})^{2} \tag{7}$$

To calculate MSE, the square of the difference between the true and predicted values is determined and then its sum is averaged. It is convenient to derive the derivative in the form of a square; consequently, this parameter is often used as the loss function of linear regression.

3. Results and discussion

The ANN model aims to study models or develop software that can mimic planned or real systems and analyze results with less effort or risk. It is helpful for predicting the potential costs and requirements of current systems, thereby achieving management with higher performance. This section first reviews the previous models used to analyze the thermophysical properties of nanofluids and then presents a comparison of the results of the simulation models that predict the thermophysical properties of carbon-based magnetofluids with those of the previous models. Finally, empirical models were developed to predict the thermophysical properties of carbon-based magnetic nanofluids, and certain possible theories are explained for the model proposed by the neural network.

3.1. Review of previous models related to theoretical thermophysical properties of nanofluids

The physical properties of nanofluids change with the addition of nanoparticles in terms of density, viscosity, thermal conductivity, and specific heat capacity [68]. Different researchers have different perspectives on how and to what extent nanoparticles affect nanofluids; however, there is no doubt that these properties are affected [55]. The consensus on the effect of thermal conductivity is that the thermal conductivity of nanofluids increases when nanoparticles are added [55,66]. However, the effect of the addition of nanoparticles on the other physical properties of nanofluids has not been investigated [69]. Several studies have been conducted on the changes caused by the addition of nanoparticles. The addition of nanoparticles may affect the properties of nanofluids in multiple ways, which can be due to the properties of nanoparticles, temperature, pH, and the amount of added nanoparticles [54-63]. Certain researchers have reported that adding nanoparticles increases the pH of the solution, but others have provided completely different results [57]. Certain researchers have indicated that the addition of nanoparticles can increase the heat capacity of nanofluids [55,61]. To accurately understand the changes in these properties, experiments are required. Several experiments have been conducted on the various physical properties of nanofluids; however, there are insufficient theoretical models for calculating the viscosity and thermal conductivity of nanofluids based on the properties of nanofluids and solutions [45,52]. The experimentally measured results are more accurate but require tools that are not very convenient.

3.1.1. Theoretical thermal conductivity models

The cooling of all types of industrial equipment is a challenging task. A variety of industrial operations, such as heating, chemical reactions, require timely cooling. There are several types of liquids used to cool equipment; however, many of the fluids used to cool the industrial equipment have poor thermal conductivity; consequently, the cooling effect is not ideal. Thermal conductivity is an important thermophysical property that is typically used to evaluate the heat transfer capability of fluids [75-92]. The Maxwell model is well known for predicting the heat conduction performance of a liquid–solid suspension. It can be applied to statistically low bulk concentrations and homogeneous mixtures in which particles are dispersed randomly and the size is uniform [75]. In the Wasp and Hamilton–Crosser models [76,77], the influence of the shape of nanoparticles on the thermal properties was considered. When compared to the classical Maxwell equation, it was revealed that the thermal conductivity can be evaluated more effectively according to the approximate method of concentration distribution of magnetic nanoparticles. Choi first proposed the role of nanoparticles in improving the thermal conductivity of liquids in 1995. Many solid substances, such as metals or nonmetallic oxides, have good thermal conductivity, and nanoparticles of these substances can improve the thermal conductivity of the liquids used for cooling. In addition to being used for equipment cooling, there is also the problem of thermal conductivity in the heat transfer process. After the nanofluid concept was introduced, an estimation process for the thermal conductivity of nanofluids in thermal exchange calculations was proposed by Yu and Choi [78], who considered the ratio of nanoparticle radius to nanolayer thickness. It was ascertained that the results of analyzing the lognormal distribution of data depend on the experimental method and the facts of the relevant model. Koo and Kleinstreuer et al. [80] demonstrated that there is a region around the nanoparticle where liquid molecules behave differently than the rest of the base fluid. This region is similar to an interfacial layer, where a transition occurs between the nanoparticle and base fluid. This affects the conductivity of the liquid. This model can be used to determine the influence of different sizes, geometries, and distributions of nanoparticles on nanofluid properties. However, this model is also limited because it is based on the premise that the mixture is continuous, and the thermal conductivity is only related to the properties of the nanoparticles and the base solution. In 2005, Chon et al. [81] proposed another correlation method for computing the effective thermal conduction performance of nanofluids at specific temperatures. It should be noted that the thermal conductivity of nanofluids decreases if an interface layer is formed. This combination is not appropriate if there is significant thermal resistance at the interface between the nanoparticle and the base solution. In fact, the liquid properties at the interface also have significant research value. Different mask properties may affect the overall thermal conductivity. Nanofluids resemble composites in their structures. If the nanofluid is analogous to a composite material, then the nanoparticle is the core, surrounded by an interfacial layer of intermediate properties, which is then surrounded by a base fluid. This structure forms a polyphase system and improves the overall thermal conductivity. Till date, extensive thermal conduction performance models have been established for nanofluids, as shown in Table 2 [75-92]. Based on previous formulas and theories, these modes consider the influences of nanoparticle size, nanoparticle shape, temperature dependence, and particle volume fraction by considering the movement of nanoparticles in the base fluid, such as Brownian motion. However, nanofluids with nanocomposites and mixture base fluids have not yet been developed, especially magnetic nanofluids in this case. Certain theories have suggested that magnetic fields result in changes in the local concentration of magnetic fluids, thereby affecting the thermal conductivity, while others have proposed that magnetic fields generate a nanoparticle chain, which can result in directional thermal enhancement.

Table 2 Summary of effective thermal conductivity models for nanofluids.

Model	Date	Equation	Remarks
Maxwell [75]	1904	$k_{eff} = k_{bf}\left[\frac{(k_{np}+2k_{bf})-2\varphi(k_{bf}-k_{np})}{(k_{np}+2k_{bf})+\varphi(k_{bf}-k_{np})}\right]$	Considered the volume fraction of solid
Hamilton and Crosser [76]	1962	$k_{eff} = k_{bf}\left[\frac{(k_{np}+(n-1)k_{bf})-(n-1)\varphi(k_{bf}-k_{np})}{(k_{np}+(n-1)k_{bf})+\varphi(k_{bf}-k_{np})}\right]$	n=3
Wasp [77]	1979	$k_{eff} = k_{bf}\left[\frac{(k_{np}+2k_{bf})-2\varphi(k_{bf}-k_{np})}{(k_{np}+2k_{bf})+\varphi(k_{bf}-k_{np})}\right]$	φ is the particles shape parameter
Yu and Choi [78]	2003	$k_{eff} = k_{bf}\left[\frac{(k_{np}+2k_{bf})-2\varphi(k_{bf}-k_{np})(1+\eta)^3}{(k_{np}+2k_{bf})+\varphi(k_{bf}-k_{np})(1+\eta)^3}\right]$	η is the ratio of the nanolayer thickness to the particle radius
Jang and Choi [79]	2004	$k_{eff} = k_{bf}\left[1 + c\frac{d_{bf}}{d_{np}}k_f\varphi Re_{d_{np}}^2 Pr\right]$	Considered the convection and conduction heat transport

Koo and Kleinstreuer [80]	2004	$k_{eff} = k_{bf}\left\{\left[\frac{(k_{np}+2k_{bf})-2\varphi(k_{bf}-k_{np})}{(k_{np}+2k_{bf})+\varphi(k_{bf}-k_{np})}\right] + 5\times10^4\beta\varphi\rho_{bf}C_{P,bf}\sqrt{\frac{K_BT}{\rho_{np}d_{np}}}f(T,\varphi)\right\}$ $f(T,\varphi) = (-134.63 + 1722.3\varphi) + (0.4705 - 6.04\varphi)\left(\frac{T}{T_0}\right)$	Considered the particle size, volume fraction and temperature dependence
Chon et al. [81]	2005	$k_{eff} = k_{bf}\left[1 + 64.7(\varphi)^{0.7640}\left(\frac{d_{bf}}{d_{np}}\right)^{0.3690}\left(\frac{k_{bf}}{k_{np}}\right)^{0.7476}Pr_T^{0.9955}Re^{1.2321}\right]$	Considered particle size and temperature
Maiga et al. [82]	2005	$k_{eff} = k_{bf}[1 + 2.72\varphi + 4.97\varphi^2]$	Considered nanoparticle volume fraction
Prasher et al. [83]	2005	$k_{eff} = k_{bf}\left\{(1 + ARe^mPr^{0.333}\varphi)\left[\frac{(k_{np}+2k_{bf})-2\varphi(k_{bf}-k_{np})}{(k_{np}+2k_{bf})+\varphi(k_{bf}-k_{np})}\right]\right\}$	Considered the convection near the particle and interfacial resistance
Patel et al. [84]	2005	$k_{eff} = k_{bf}\left\{1 + \frac{k_{np}d_{bf}\varphi}{k_{bf}d_{np}(1-\varphi)}\left[1 + c\frac{2K_BTd_{np}}{\pi\alpha_{bf}\mu_{bf}{d_{np}}^2}\right]\right\}$	Considered the nanoparticle diameter, volume concentration and Brownian motion
Timofeeva et al. [85]	2009	$k_{eff} = k_{bf}[1 + (C_k^{shape} + C_k^{surface})\varphi] = k_{bf}[1 + C_k]$	Considered the nanoparticle shape
Vajjha et al. [86]	2010	$k_{eff} = \left[\frac{(k_{np}+2k_{bf})-2\varphi(k_{bf}-k_{np})}{(k_{np}+2k_{bf})+\varphi(k_{bf}-k_{np})}\right]k_{bf} + 5\times10^4\beta\varphi\rho_{bf}C_{P,bf}\sqrt{\frac{K_BT}{\rho_{np}d_{np}}}f(T,\varphi)$ $f(T,\varphi) = (2.8217 * 10^{-2}\varphi + 3.917 * 10^{-3})\left(\frac{T}{T_0}\right) + (-3.0669 * 10^{-2}\varphi -$ $3.3.91123 * 10^{-3})$	Considered the nanoparticle diameter, volume concentration and Brownian motion
Corcione et al. [87]	2011	$k_{eff} = k_{bf}\left[1 + 4.4Re_{np}^{0.4}Pr_{bf}^{0.66}\left(\frac{T}{T_{fr}}\right)^{10}\left(\frac{k_{np}}{k_{bf}}\right)^{0.03}\varphi^{0.66}\right]$ $Re_{np} = \frac{2\rho_{bf}K_BT}{\pi{\mu_{bf}}^2d_{np}}$	Considered the frizzing point of base fluid ($0.2\% \leq \varphi \leq 9\%$)
Nkurikiyimfura et al. [88]	2013	$k_{eff} = k_{bf}[(3\varphi_{int} - 1) + 3(1 - \varphi_{int}) + [(3\varphi_{int} - 1) - 1]^2]$	Considered the magnetism parameter
Sharma et al. [89]	2014	$k_{eff} = k_{bf}\left[0.8938\left(1 + \frac{\varphi}{100}\right)^{1.37}\left(1 + \frac{T}{70}\right)^{0.2777}\left(1 +\right.\right.$ $\left.\left.\frac{d_{np}}{150}\right)^{-0.0336}\left(\frac{\alpha_{np}}{\alpha_{bf}}\right)^{0.01737}\right]$	Considered the different components in the nanofluids
Sundar et al. [90]	2014	$k_{eff} = k_{bf}[A + B\varphi]$	Considered the nanoparticle diameter, volume concentration temperature and thermal diffusivity
Esfe et al. [91]	2015	$k_{eff} = k_{bf}[1 + (0.26876 \times \varphi^{0.99288} \times {d_{np}}^{-0.35106})]$	Fe-H_2O
Hassani et el. [92]	2015	$k_{eff} = k_{bf}\left\{1.04 + \varphi^{1.11}\varphi^{0.99288}\left(\frac{k_{np}}{k_{bf}}\right)^{0.33} \times Pr^{-1.7}\left[\frac{1}{Pr^{-1.7}} - \frac{262}{\left(\frac{k_{np}}{k_{bf}}\right)^{0.33}} +\right.\right.$ $\left.\left.\left(135\left(\frac{d_{ref}}{k_{np}}\right)^{0.23}\left(\frac{v_{bf}}{d_{np}v_{Br}}\right)^{0.82}\left(\frac{C_P}{T^{-1}{v_{Br}}^2}\right)^{-0.1}\left(\frac{T_{bf}}{k_{np}}\right)^{-7}\right)\right]\right\}$	Considered Brownian velocity and molecular diameter of hydrogen

3.1.2. Theoretical prediction models of viscosity

While considering the viscosity of nanofluids, there are several published theoretical models for predicting the viscosity, as listed in **Table 3** [82,85,87,89-101]. They summarized the effects of several property parameters of nanoparticles on the dynamic viscosity of nanofluids. These parameters include temperature and the shape of the particles. This shows that the addition of nanoparticles affects the viscosity of the liquid; moreover, as more nanoparticles are added, the increase in viscosity becomes greater. Further, as the temperature of the particle increases, the degree of viscosity increases. Although several factors influence the viscosity of nanofluids, correlations can still be identified. Till date, all the predicted modes indicate that temperature and concentration are two important factors affecting the viscosity of nanofluids. Different studies have proposed different theoretical models according to the volume concentration and temperature range, but there is no unified model with wider adaptability. For instance, Koo and Kleinstreuer et al. [96] considered the effect that results from the Brownian motion of nanoparticles in low volume concentrations. When the volume concentration is greater than a certain value, the model underestimates the valid suspension viscosity because it reckons without considering the interaction between particles. Certain extended correlations for the case of higher nanoparticle fractions were also proposed based on the notional analysis. Nguyen et al. [97] presented a simple correlation based on experiments that considered high volume concentrations of nanoparticles. When the volume fraction further increases, certain studies consider the Krieger–Dougherty equation using the intrinsic viscosity and effective volume concentration. This model is widely used to forecast the valid viscosity of liquid–solid suspensions. Nevertheless, it is applicable in the case of low volume concentrations. In the case of the effect of temperature on nanofluid viscosity, Abu-Nada [98] predicted that the influence of temperature on the viscosity of the base fluid is approximately equivalent to its influence on the viscosity of the nanofluid. Certain definitions of the relationship between these two factors and the viscosity of nanofluids were proposed by Masoumi et al. They introduced magnetism into the viscosity of nanofluids. Their study identified that a fluid with magnetism, with or without an applied magnetic field, is more viscous than before. Here, the strength and direction of the magnetic field are the key factors. Saedodin et al. [100] proposed a theory within a dimensionless group in terms of bulk concentration, nanoparticle size, and temperature to calculate the effective viscosity of a nanofluid. Because the magnetic field blocks the motion of the particles, it can stop the movement of particles. The exact mechanism of this phenomenon is not yet clear, and further experiments and exploration are required. Moreover, Esfe et al. [101] believe this is because magnetic fields that are perpendicular to the fluid are more viscous than fields that are parallel to the fluid. This will allow the reader to have a more contradictory understanding. It is worth mentioning that Wang et al. developed a viscosity model of magnetic nanofluids by considering magnetic field intensity, temperature, and concentration. When the direction of the magnetic field is parallel or perpendicular to the direction of the fluid, the viscosity of the fluid also increases with an increase in the strength of the magnetic field, and the two are positively correlated. However, when the magnetic field increases to a certain strength, the viscosity of the fluid stabilizes, rather than increasing continuously. There are certain differences in the available data regarding the increase in fluid viscosity owing to the two different directions. Despite these works, the viscosity of composite-based nanofluids under applied magnetism has not been researched.

Table 3 Summary of effective dynamic viscosity models for nanofluids.

Model	Date	Equation	Remarks
Pak and Cho [95]	1998	$\mu_{eff} = \mu_{bf}[1 + 39.11\varphi + 533.9\varphi^2]$	Water-Al_2O_3 nanofluids Water-TiO_2 nanofluids
Maiga et al. [82]	2005	$\mu_{eff} = \mu_{bf}[1 + 7.3\varphi + 123\varphi^2]$ $\mu_{eff} = \mu_{bf}[1 - 0.19\varphi + 306\varphi^2]$	Water-Al_2O_3 nanofluids Ethylene glycol-Al_2O_3 nanofluids
Koo and Kleinstreuer [96]	2005	$\mu_{eff} = \frac{\mu_{bf}}{(1-\phi)^{2.5}} + \mu_{Brownian}$ $\mu_{Brownian} = 5 \times 10^4 \beta\varphi\rho_{bf}\sqrt{\frac{K_B T}{\rho_{np} d_{np}}} f(T,\varphi)$ $f(T,\varphi) = (-134.63 + 1722.3\varphi) + (0.4705 - 6.04\varphi)\left(\frac{T}{T_0}\right)$ $\beta = \begin{cases} 0.0137(100\varphi)^{-0.8229}, \varphi < 0.01 \\ 0.0011(100\varphi)^{-0.7272}, \varphi > 0.01 \end{cases}$	Water-CuO nanofluid $1\% \leq \varphi \leq 4\%$ $300K < T < 325K$ Water-Al_2O_3 nanofluids
Nguyen et al. [97]	2007	$\mu_{eff} = \mu_{bf}[0.904e^{0.148\varphi}],\ d_{np} = 47nm$ $\mu_{eff} = \mu_{bf}[1 + 0.025\varphi + 0.015\varphi^2], d_{np} = 36nm$ $\mu_{eff} = \mu_{bf}[1.475 - 0.319\varphi + 0.051\varphi^2 + 0.009\varphi^3], d = 29nm$	CuO/water nanofluid $1\% \leq \varphi \leq 13\%$ $T = 295K$
Abu-Nada [98]	2009	$\mu_{eff} = -0.155 - \frac{19.582}{T} + 0.794\varphi + \frac{2094.47}{T^2} - 0.192\varphi^2 - \frac{8.11\varphi}{T} - \frac{27463.863}{T^3} + 0.0127\varphi^3 + \frac{1.6044\varphi^2}{T} + \frac{2.175\varphi}{T^2}$	Considering the effect of temperature of nanofluids; $1\% \leq \varphi \leq 9.4\%$; $295K < T < 348K$
Masoumi et al. [99]	2009	$\mu_{eff} = \mu_{bf} + \frac{\rho_{bf} V_B d_{np}^2}{72C\delta}$ $\delta = \sqrt[3]{\frac{\pi}{6\varphi}} d_{np},\ V_B = \frac{1}{d_{np}}\sqrt{\frac{18k_{bf}T}{\pi\rho_{np}d_{np}}}, C = \mu_{bf}{}^{-1}(a\varphi + b)$	Al_2O_3($13nm, 28nm$)/water nanofluids
Timofeeva et al. [85]	2009	$\mu_{eff} = \mu_{bf}(1 + A_1\varphi + A_2\varphi^2)$	Nonspherical nanoparticles (platelet, blade, cylinder, and brick)
Corcione [87]	2011	$\mu_{eff} = \mu_{bf}\left[\frac{1}{\left(1-34.87(d_{np}/d_{bf})^{-0.3}\varphi^{1.03}\right)}\right]$ $d_f = 0.1\left(\frac{6M}{N\pi\rho_{bf0}}\right)^{1/3}$	For oxide and metal nanoparticles suspended in water or ethylene glycol based nanofluids $0.2\% \leq \varphi \leq 9$
Esfe and Saedodin [100]	2014	$\mu_{eff} = \mu_{bf}[0.9118Exp(5.49\varphi - 0.00001359T^2) + 0.0303Ln(T)]$	ZnO/EG; $0.25\% \leq \varphi \leq 5\%$ $298K < T < 323K$
Esfe et al. [101]	2014	$\mu_{eff} = \mu_{bf}[1 + 11.61\varphi + 109\varphi^2]$	$0.0625\% \leq \varphi \leq 1\%$
Sharma et al. [89]	2014	$\mu_{eff} = \mu_{bf}\left[\left(1 + \frac{\varphi}{100}\right)^{11.3}\left(1 + \frac{T}{70}\right)^{-0.038}\left(1 + \frac{d_{np}}{170}\right)^{-0.061}\right]$	$0\% \leq \varphi \leq 4\%$ $20nm < d_{np} < 150nm$ $293K < T < 343K$

Sundar et al. [90]	2014	$\mu_{eff} = \mu_{bf}[Ae^{B\varphi}]$	$(0.3\% \leq \varphi \leq 1.5\%)$ $(293K < T < 333K)$
Esfe et al. [91]	2015	$\mu_{eff} = \mu_{bf}[1 + (0.100 \times \varphi^{0.69574} \times d_{np}{}^{0.44708})]$	Fe/water$(37nm, 71nm, 98nm)$ $0.0313\% \leq \varphi \leq 1\%$
Wang et al. [102]	2016	$\mu_{eff} = e^{-0.02T}[0.035H^2 + 3.1H - 27886\varphi^2 + 4263\varphi + 316]$	Temperature (*T*), magnetic field (*H*), and concentration (φ)

3.1.3. Theoretical prediction models of specific heat

For energy storage materials, especially phase change materials for heat storage, the parameter of specific heat has attracted considerable attention as it changes significantly with temperature. In nanofluids, the specific heat appears to be a weaker characteristic when compared to the thermal conductivity and viscosity of nanofluids because solid–liquid specific heat models that are stable over a large temperature range have been regarded as the criterion since they were proposed. The first assumption is that, by the mixing rule, the specific heat of the entire mixture is a combination of the specific heat of the individual components. However, according to the experimental results, the results obtained using this assumption were rather large. The second hypothesis is that there is thermal equilibrium between the nanoparticles and the base solution. Pak and Cho et al. [95] conducted viscosity measurements using a rotating viscometer and proposed a mathematical model by analyzing the specific heat of two different nanofluids. It was calculated considering the volume concentration, density, and average bulk temperature. In this century, models for determining nanofluid specific heat by temperature and concentration have been gradually developed, although temperature has a lesser effect on the nanofluid specific heat when compared to nanofluid concentration. Maiga et al. [82] showed that the suspension rheology results were significantly larger than the classical viscosity. Their work studied the specific heat of nanofluids from the perspective of molecular structure and mechanics. The experimental results show that nanofluids have stable specific heat at a certain temperature, and the length, diameter, and chirality of nanofluids do not affect the specific heat. Vajjha and Das et al. [103] proposed a viscosity mode by summarizing experimental research on different nanofluids. The results indicated that the specific heat of the base fluid and nanofluid had similar performances in the specific heat of bulk graphite powder. The aligned nanofluid specific heat was smaller and less dependent on temperature than the bulk in an environment with temperature higher than the room temperature. Pakdaman et al. [104] used the modulated temperature differential scanning calorimetry technique to determine the specific heat and reported a good agreement between the obtained and tabulated values of the constituting components of nanofluids. According to the experimental results, if nanoparticles are added, certain changes will occur in the crystallization and melting processes of the base solution. Within the scope of this study, it was determined that Cu nanoparticles affected the base solution by reducing its specific heat. Ghazvini et al. [105] proposed that the specific heat can be influenced by the nanoparticle type and different factors such as temperature, base fluid, and volume fraction. Moreover, Shin and Banerjee et al. [23] researched suspension-specific heat based on the thermal equilibrium assumption of salt eutectics. In 2015, Sharma and Sekhar [38] predicted the specific heat with the assumption of an infinitely dilute liquid mixture by adding spherical solid particles. They proposed three related parameters (temperature, concentration, and nanoparticle size) that can change the physical properties of nanofluids. The results of the experiment on the specific heat capacity of nanofluids measured using a differential scanning calorimeter showed that the size of nanoparticles had minimal effect on the ability of nanoparticles to improve the specific heat of nanofluids. The experimental results show that the specific heat of the base solution decreases after the addition of nanoparticles; moreover, with the increase in the added nanoparticles, the specific heat of the base solution decreases gradually. These models are summarized as follows.

Table 4 Summary of effective specific heat models for nanofluids

Model	**Date**	**Equation**	**Remarks**
Pak and Cho [95]	1998	$C_{p-cp}=\frac{1}{\gamma^3}C_{p-p}+\left(1-\frac{1}{\gamma^3}\right)\left\{\frac{3C_{p-p}}{pb'^3}\left(2t^2+2b'r_pt+b'^2r_p^2\right)-\frac{3C_{p-f}}{pb'^3}\left[t^2\left(2+2b'+b'^2\right)+b'r_p\left(b'r_p+2b't+2t\right)\right]\right\}$	Water-Al_2O_3 nanofluids Water-TiO_2 nanofluids
Maiga et al. [82]	2005	$C_{p,hnf}=\varphi_{np1}C_{p,np1}+\varphi_{np2}C_{p,np2}+\frac{\left(1-\varphi_{np1}-\varphi_{np2}\right)C_{p,bf}}{\rho_{hnf}}$	Water-Al_2O_3 nanofluids Ethylene glycol-Al_2O_3 nanofluids
Vajjha and das et al [103]	2009	$C_{p,nf}=C_{p,bf}\frac{\left(AT+BC_{p,np}/C_{p,bf}\right)}{(C+\varphi)}$	A, B, C are different values
Pakdaman et al. [104]	2012	$C_{p,nf}-C_{p,bf}=C_{p,bf}(AT+B)wt^c$	A, B, C are linked with different nanofluids
Ghazvini et al. [105]	2012	$C_{p,nf}=C_{p,bf}(A+BT+CT^2)$	A, B, C are linked with different factors
Shin and Banerjee [23]	2014	$C_{p,nf}=C_{p,bf}\frac{\rho_{ns}C_{p,ns}\varphi_{ns}+\rho_sC_{p,s}\varphi_s+\rho_{np}C_{p,np}\varphi_{np}}{\rho_{ns}\varphi_{ns}+\rho_s\varphi_s+\rho_{np}\varphi_{np}}$	Alkali carbonate-Al_2O_3 salt eutectics
Sharma and Sekhar [38]	2015	$C_{p,nf}=0.843C_{p,bf}\left(1+\frac{T_{nf}}{50}\right)^{-0.304}\left(1+\frac{d_{np}}{50}\right)^{0.417}\left(1+\frac{\varphi}{100}\right)^{2.272}$	Al_2O_3 and SiO_2, etc. $15<d_{np}<50$, $20<T<50$, $0.01<\varphi<4$

3.2. Model verification and evaluation of ANNs

However, unitive theoretical formulas for predicting the dependence of the viscosity of nanofluids on mass concentration, temperature, and magnetism are insufficient [106-112]. An ANN is proposed to cope with the nonlinear fitting in this work on the basis of experimental results [113,114]. The Pearson correlation coefficients of the input and output parameters are listed in **Table** 5. It can be observed that there is a significant correlation between the input and output parameters. Then, the performance of the trained ANN model was tested using the training data. The results predicted using the ANN model were compared with the experimental data of carbon-based magnetic nanofluids. During the learning course of the ANN model (spread=1), the accuracy of training was considered to be acceptable if the evaluation index error conformed to the required tolerance. If not, hidden layer nodes were added and the routine was rerun [115-117]. On this basis, the number of hidden layers was analyzed to determine the final prediction model. **Fig. 8** illustrates the transformation of the four evaluation indices when the number of hidden layer nodes were increased from 5 to 11 based on the statistical coefficient values of error indicators or multiple determinations. This suggests that more nodes must be considered to improve the predicted accuracy. The 10-node model demonstrated better prediction performance than other models for carbon-based magnetic nanofluids while also considering the computational efficiency.

Table 5 The Pearson correlation coefficient (PCC) of the input and output parameters

Pearson correlation coefficient (PCC)		Input parameters				
		φ_m	φ_e	φ_n	T	M
Output parameters	k	0.6610	0.7921	0.7426	0.8233	0.8961
	μ	0.7900	0.7179	0.9501	0.7846	0.8822
	C_p	0.9207	0.9572	0.9246	0.5464	0.5053

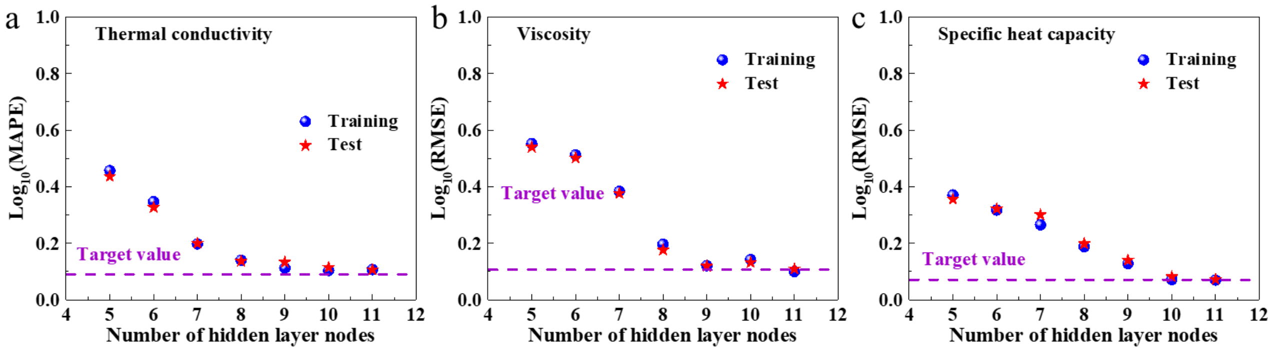

Fig. 8 The MAPE evaluation of artificial neural networks for predicting thermo-physical properties (thermal conductivity, viscosity, specific heat capacity) of carbon-based magnetic nanofluid

Owing to the small dataset (713 data items), the batch size should not be too large, and it should be reduced if memory constraints occur [118-120]. The number of epochs was divided into six stages; each stage was 50, and the initial learning rate was 10. After each stage, the learning rate was reduced for the next stage [118,119]. After debugging, the convergence speed was the fastest under the parameters listed in **Table 6**. The results showed good agreement (within the ±5% error) between the experimental and predicted viscosities of carbon-based magnetic suspensions. The effect of certain hyperparameters on the output of the network was determined by sensitivity analysis [120]. Hence, the most effective hyperparameters can be selected to improve the output [121-124]. The ANN model possesses a superior modeling ability to predict the suspension viscosity, which is based on the output-input experimental data [123]. It can be noted that the ANN model with temperature as its input variable has a better prediction performance for carbon-based magnetic nanofluids. For the testing samples, a comparison of the data predicted by the ANN model and the experimental data of carbon-based magnetic nanofluids is illustrated in **Fig. 9**. The standard deviation demonstrates that the thermophysical properties are almost similar to the test results, and it measures the variation in the model values.

Table 6 The features and parameters of ANN models used in this work

Neurons	Batch Size	Epoch	Learning rate	Decay coefficient
10	4	50	0.0001	5

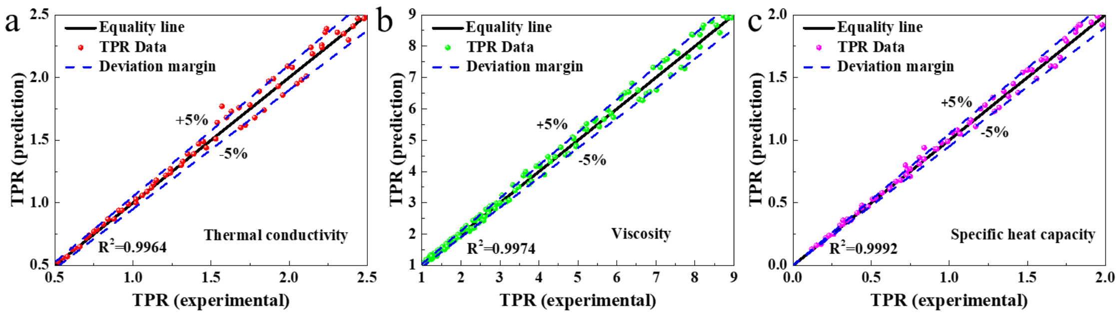

Fig. 9 Comparison of experimental and predicted thermo-physical properties of carbon-based magnetic nanofluid: (a) Thermal conductivity; (b) Viscosity; (c) Specific heat capacity

3.3. Comparison of ANN model with existing predicted models

The purpose of data analysis is to use logical and statistical methods to assist in interpreting, summarizing, and evaluating data [125,126]. Normalization coefficients were used to determine the effect of the respective variables on the value of the dependent variable [127,128]. As previously mentioned, empirical correlations and theoretical models have also been developed. In this work, the established thermophysical properties using the ANN model is used to analyze the effects of different factors (such as nanoparticle volume concentration, temperature, and nanoparticle size) on the viscosity of nanofluids in comparison with the theoretical models [129]. **Figs. 10-12** show the comparisons between the thermophysical properties predicted using the ANN models and the experimental data, as well as the functional values within the influence factors of other models that predict the thermophysical properties of carbon-based magnetic nanofluids after normalization. From **Fig. 10a**, it can be noted that the predicted values obtained using both the Maxwell and Timofeeva models are lower than the experimental data, which may be because these models do not consider effects other than the shape and volume concentration of the nanoparticles. **Fig. 10b** illustrates the enhancement of thermal conductivity with the increase in temperature, and it can be observed that the prediction result of the ANN model with the increase in temperature is closer to the experimental value than the other models. Recent investigations have proven that scientists have attempted to control the thermal conductivity of magnetic nanofluids under the influence of external forces such as magnetic fields, sound fields, and electric fields. This may be an important reason for the recent increased interest in enhancing the thermal conductivity of magnetic nanofluids. Nkurikiyimfura et al. [88] indirectly proposed a formula for thermal conductivity by considering the interaction energy with the local magnetic field. When compared to his model, as shown in **Fig. 10c**, the ANN model can accurately predict the trend of nanofluid thermal conductivity with better results under varying magnetic field intensities. The data deviation predicted by the ANN model relative to the experimental data was smaller than that of the other models (**Figs. 10a-c**). These results indicate that the ANN model has better prediction performance for the thermal conductivity of carbon-based magnetic nanofluids than other models. Meanwhile, it was indicated that when the temperature changed, the difference between the experimental and predicted values was small, whereas, when the magnetic field changed, the difference between the experimental and predicted values was large.

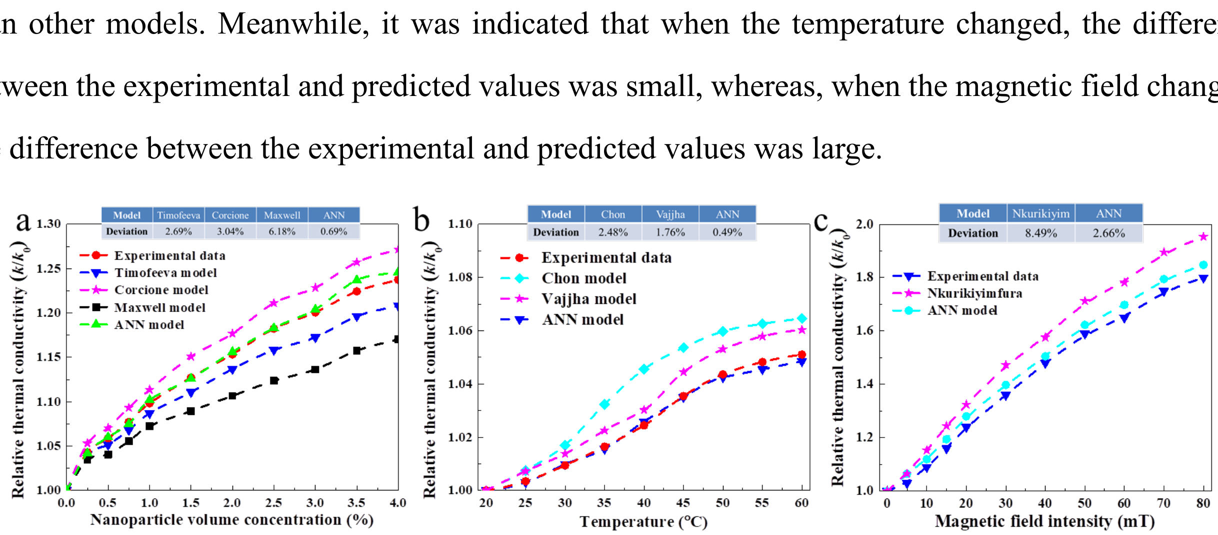

Fig. 10 The effect comparison of (a) nanoparticle volume concentration, (b) temperature, and (c) magnetic field intensity on thermal conductivity of carbon-based magnetic nanofluid between various model and experimental data

The same analysis was also performed for the viscosity of carbon-based magnetic nanofluids. **Fig. 11** compares the prediction of viscosity based on different models with the experimental results for the carbon-based magnetic nanofluids as functions of solid volume concentration, temperature, and magnetic field intensity. **Fig. 11a** shows the comparisons between the results of the ANN model and the predicted data of other models. Thus, it can be observed that the viscosity of carbon-based magnetic nanofluids depends significantly on the solid volume concentration. As the concentration increases, the nanoparticles in the suspension enhanced the internal shear effect, leading to an increase in the viscosity of the nanofluid. It can also be observed that the prediction result of the ANN model with a tendency of variation in concentration is more accurate than the experimental value. These models only obtain the changes in the viscosity of the nanofluid based on the influence of temperature. It can be concluded from **Fig. 11b** that the ANN model could achieve a superior prediction performance for viscosity when considering the effect of temperature. **Fig. 11c** compares the experimental measurements with the predicted viscosity under a magnetic field using the ANN model. For the Wang model [102], the additional effects of the magnetic field are directly considered in viscosity modeling. All the above statements indicate that the prediction of experimental data by other models is significantly lower than that of the ANN model and its experimental data, which further illustrates that the ANN model can be successfully used to assess the viscosity of carbon-based magnetic nanofluids. When compared to all the prediction results of the ANN model, the predicted viscosity under the magnetic field has the highest data deviation (4.97%), which is less than ±5%. This further illustrates that the ANN model can be successfully used to predict the viscosity of carbon-based magnetic nanofluids.

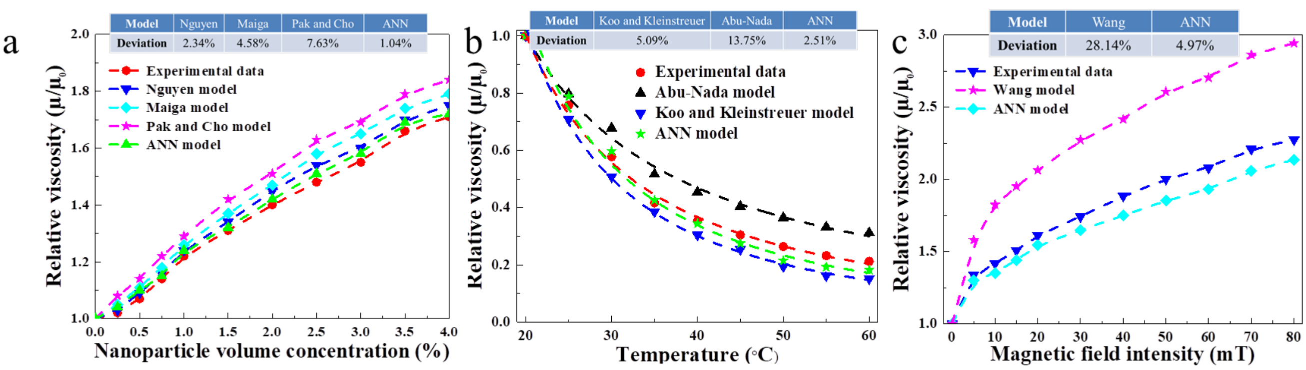

Fig. 11 The effect comparison of (a) nanoparticle volume concentration, (b) temperature, and (c) magnetic field intensity on viscosity of carbon-based magnetic nanofluid between various model and experimental data.

The present study provides useful information about the specific heat of magnetic nanofluids under a magnetic field. An ANN model was established to forecast the specific heat by considering the temperature, nanoparticle concentration, and magnetic intensities based on experimental results. As shown in **Fig. 12**, the specific heat of carbon-based magnetic nanofluids decreased with the increase in solid particle concentration and slowly increased with the increase in temperature. When compared to the temperature and magnetic field, volume concentration performs a more important role in the specific heat of carbon-based magnetic nanofluids because it satisfies the bulk average value in mathematics. Hence, the change in the specific heat is still not obvious with a low solid volume concentration. Most models that contained an ANN model assumed that the specific heat capacity of the nanofluids increased slowly with increase in temperature and the increase could even be negligible, which is consistent with the experimental results. The data deviation predicted by the ANN model relative to the experimental specific heat capacity data under a magnetic field was 0.01%, which is the closest experimental value among all the predictions. Because the measurement is the average specific heat capacity in volume, previous models, including this work, indicated that the magnetic field primarily affects the magnetic nanofluid thermal conductivity and viscosity, but has little influence on the specific heat capacity. When compared to the thermal conductivity and viscosity, the data deviation of the specific heat capacity predicted by the ANN model is smaller owing to the stability of this parameter.

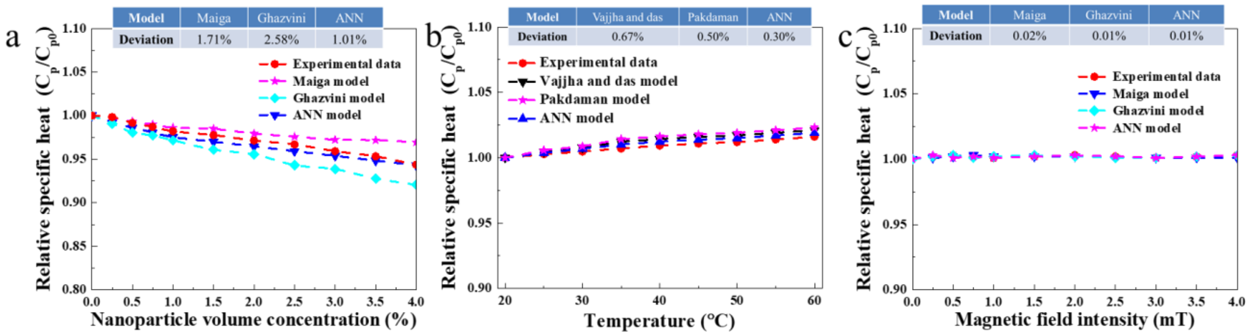

Fig. 12 The effect comparison of nanoparticle volume concentration, temperature, and magnetic field intensity on specific heat of carbon-based magnetic nanofluid between various model and experimental data

4. Application, challenges, and prospects

4.1. Application of magnetic nanofluids

4.1.1 Applying magnetic nanofluids in a heat exchanger

Magnetohydrodynamics has attracted considerable interest because of its potential in the flow control of mini-devices and heat dissipation of electronic components [9,130,131]. Owing to their flexible and superparamagnetic properties, magnetic nanofluids are employed not only as tunable templates for the fabrication of orderly lined microarrays, but also as carrier solutions for heat and mass transport under an external magnetic field in thermal management devices [9]. From the perspective of materials, the thermophysical properties of nanofluids can be controlled based on parameters such as the type and diameter of nanoparticles. Meanwhile, the heat flux and force acting on nanofluids can be tuned through gravity, pumps, and capillarity forces [130]. Till date, the idea of precise manipulation has been developed for the continuous generation of magnetic or electrical droplets and nanofluids controlled by an external field [9,130]. Based on this, devices can be designed within the function to open or close thermal fluxes, thereby controlling the direction and intensity of the heat flux. Thus, remote heat and mass transport under an external field in thermal management devices can be achieved [131].

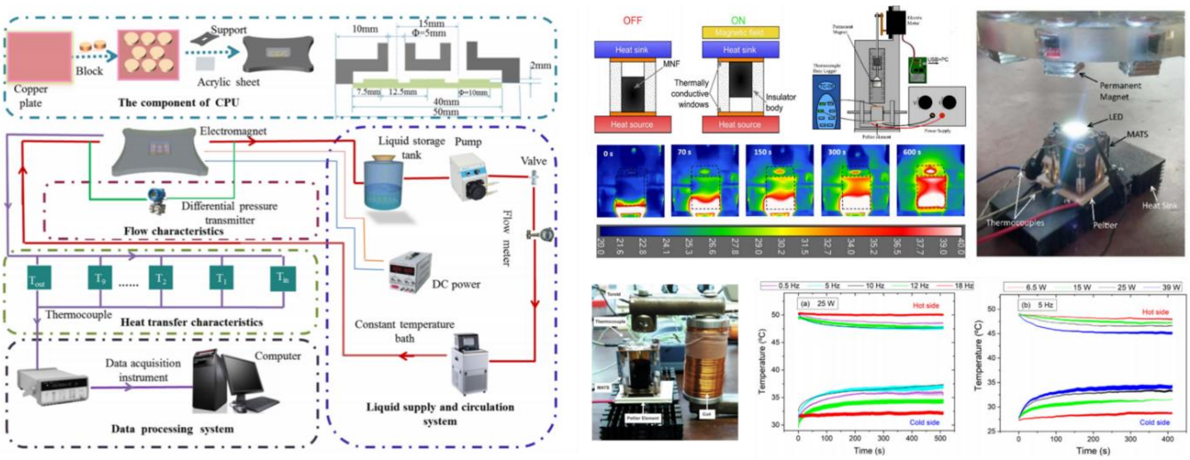

Fig. 13 (a) A cooling system designed to explore the thermo and hydraulic behaviors of magnetic nanofluids in CPU; (b) A magnetically-activated heat exchanger with remote activation based on magnetic nanofluids; (c) A magnetically driven thermal exchanger without moving parts

4.1.2 Applying magnetic nanofluids in fluid mechanics

The semi-active control achieved by the magnetorheological damping effect has been widely used in the fields of automobile manufacturing [4], hydraulic control [132], and robotics [130]. The magnetic nanofluid is maintained in the region with the strongest magnetic field without an external force. Under the action of external force, the position and shape of the magnetic fluid change, resulting in a change in the magnetic field force, and the magnetic field force is balanced with the external force, resulting in a new equilibrium state for the magnetic fluid. Based on this principle, a magnetic nanofluid seal was used to protect key components [132]. As a new type of lubricant, it can maintain the liquid at the lubrication part, and even change the pressure distribution of the polishing pad under the action of an external magnetic field, which satisfies the requirements for the workpiece during the sealing process [133].

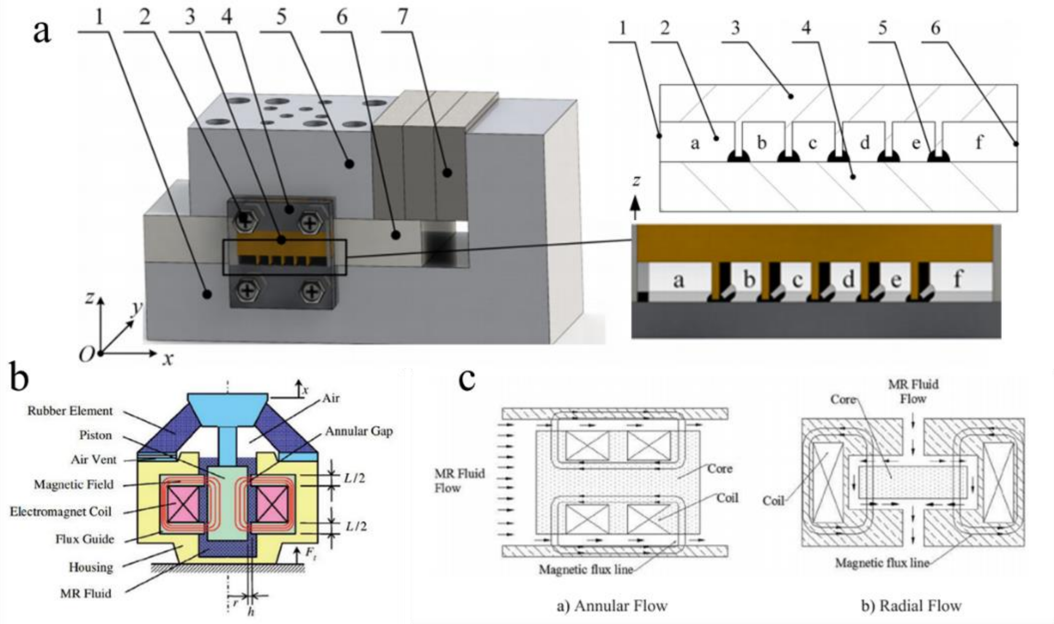

Fig. 14 (a) Structure of the planar multitooth magnetic fluid seal [132]; (b) Schematic diagram of the magnetorheological mount using magnetorheological seal structure with external coil; (c) Annular and radial flow [133]

4.1.3 Applying magnetic nanofluids in micro-nano devices

Droplet manipulation and microfluidic control are emerging as promising tools in various applications, including physics, medicine, and engineering, owing to the development of microfluidic chips [134]. However, conventional methods of controlling fluids are inadequate in satisfying the changing demands of technology and industries. Magnetic nanofluid is one of the key control components in the manipulation of droplets and fluids owing to its outstanding features, such as rapid magnetic reaction, flexible flowability, and thermal properties [135]. In recent years, magnetic microfluidic systems have developed rapidly and are regarded as an indispensable branch of microfluidics. Magnetic microfluidics can be divided into continuous-flow and digital magnetic microfluidics, which harness magnetic fields as actuators and magnetic materials as driven objects [136-139]. Magnetic microfluidics not only inherits systematic and precise control over individual fluids and droplets of traditional microfluidics but is also characterized by a simple actuation strategy, flexible controllability, remote operation, and noninvasive manipulation ability [140].

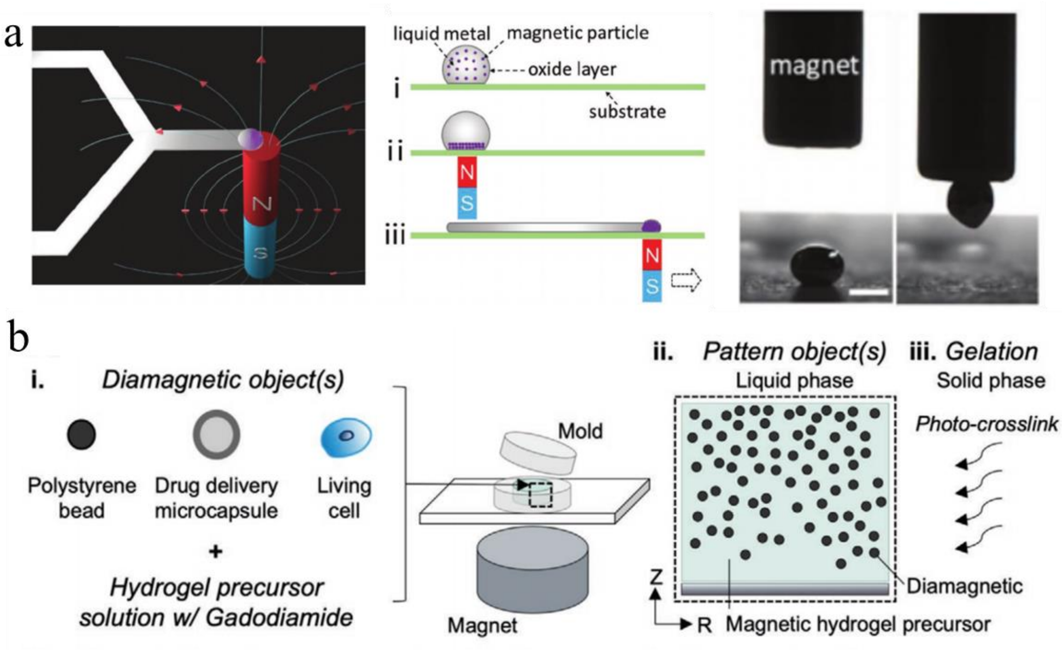

Fig. 15 (a) Schematic illustration of the direct patterning of liquid metal using magnetic field and detailed operation steps for the patterning [134]; (b) Schematic of magneto-patterning setup with the application of the magnetic field [135]

4.2. Challenges and prospects of magnetic nanofluids

This current ANN model could be continuously developed and the database content can be enriched, which can ensure more accurate prediction results when compared to the experimental data [146,147]. The use of magnetic nanofluids in heat transfer applications is promising [148]. Certain investigations of flow heat transfer, such as the enhancement of thermal conductivity based on magnetic nanofluids, were discussed under an external magnetic field [149,150]. In fact, magnetic control of liquid flow opens new possibilities in the field of microfluidics, allowing new channel shapes and low-pressure cargo transport to surpass the current capabilities of standard methods [151-155]. It promises low-shear flow and pumping, which is of growing importance in thermal management [155], fluid mechanics [154], and micro-nano devices [36]. However, there is still a lack of systematic research on the preparation of magnetic nanoparticles, magnetohydrodynamic thermophysical characteristics of nanofluids, and microflow heat switch applications [156]. In particular, there is still a lack of a prediction model for thermophysical properties of magnetic nanofluids that considers magnetic field intensity, temperature, and concentration [93,156]. Based on this, certain studies are still required to develop and explore the following aspects.

a) To prepare magnetic nanoparticles with controllable morphology and then investigate the magnetic nanofluids and droplet manipulation techniques through experiments.

b) To determine the thermophysical properties of the nanofluid under a magnetic field. The thermophysical properties of the prepared magnetic nanofluids were experimentally characterized under a dynamic magnetic field.
c) To establish a multiphysics numerical model that precisely describes the magnetic response processes of heat release and storage. Based on this, the magnetohydrodynamic heat transfer can be fully understood.
d) To establish a dynamic magnetic-response thermophysical model based on machine learning, which can provide a precise description of the magnetic field on the thermophysical properties of magnetic nanofluids using a low-cost and time-saving method.
e) To provide a noncontact control method for microflow and heat transfer. Potential applications could be verified and explored, such as wettability manipulation, drug delivery, and heat sinking.

5. Conclusion

In this study, the specific heat capacity, thermal conductivity, and viscosity of carbon-based magnetic nanofluids were measured for different magnetic volume fractions in nanomaterials, organic mass fractions in the base fluid, nanomaterial volume fractions in the nanofluid, temperatures, and magnetic field strengths. Then, the thermophysical properties of the previous measurement results of carbon-based magnetic nanofluids were reviewed. Based on these experimental data, an ANN was established and a comparison was performed with the experimental results. A minireview of previous models of nanofluid thermophysical properties was presented. Meanwhile, the proposed ANN model can obtain a lower statistical error index and a higher multiple decision statistical coefficient. The comparative results showed that there were deviations of ±5% for the ANN from the experimental data. It was identified from comparisons that the optimal ANN model is more accurate in predicting the thermophysical properties of carbon-based magnetic nanofluids than other models, and certain possible theories were explained for the model proposed by the neural network. It should also be noted that the major limitations associated with ANN applications are the requirement of a large number of parameters and lack of parameter selection methods. To conclude, this work summarized the thermophysical properties of carbon-based magnetic fluids and discussed their applications and prospects. It established a neural network model for predicting the thermophysical properties of magnetic nanofluids and proposed a method that uses material informatics to study functional materials.

References

[1] Vanaki S, Ganesan P, Mohammed H. Numerical study of convective heat transfer of nanofluid: A review, Renewable and Sustainable Energy Reviews 2016; 54: 1212-1239.

[2] Pinto RV, Augusto F, Fiorelli S. Review of the mechanisms responsible for heat transfer enhancement using nanofluids. Applied Thermal Engineering 2016; 108: 720-739.

[3] Xu B, Liu L, Lim H, Qiao Y, Chen X. Harvesting energy from low-grade heat based on nanofluids. Nano Energy 2012; 1(6): 805-811.

[4] Lv P, Liu C, Rao Z. Review on clay mineral-based form-stable phase change materials: preparation, characterization and applications. Renewable & Sustainable Energy Reviews 2017; 68: 707-726.

[5] Azmi WH, Sharma KV, Mamat R, Najafi R, Mohamad MS. The enhancement of effective thermal conductivity and effective dynamic viscosity of nanofluids-a review. Renewable & Sustainable Energy Reviews 2016; 52: 1046-1058.

[6] Zhai X, Qi C, Yang Y, Wang J. Thermo-hydraulic performance of nanofluids under adjustable magnetic field. Applied Thermal Engineering 2021; 186:116491.

[7] Nkurikiyimfura I, Wang Y, Pan Z. Heat transfer enhancement by magnetic nanofluids-A review, Renewable & Sustainable Energy Reviews 2013; 21: 548-561.

[8] Hu Y, He Y, Zhang Z, Wen D. Effect of Al_2O_3 nanoparticle dispersion on the specific heat capacity of a eutectic binary nitrate salt for solar power applications. Energy Conversion and Management 2017; 142: 366-373.

[9] Qi, C, Tang J, Fan F, Yan Y. Effects of magnetic field on thermo-hydraulic behaviors of magnetic nanofluids in CPU cooling system. Applied Thermal Engineering 2020; 179: 115717.

[10] McGrail BP, Thallapally PK, Blanchard J, Nune SK, Jenks JJ, Dang LX. Metal-organic heat carrier nanofluids. Nano Energy 2013; 2(5): 845-855.

[11] Zhu T, Cheng R, Sheppard GR, Locklin J, Mao L. Magnetic-field-assisted fabrication and manipulation of nonspherical polymer particles in ferro fluid-based droplet micro fluidics. Langmuir 2015; 8531-8534.

[12] Liu Y, Wang X, Wu H. High-performance wastewater treatment based on reusable functional photo-absorbers. Chemical Engineering Journal 2017; 309: 787-794.

[13] Shi L, He Y, Wang X, Hu Y. Recyclable photo-thermal conversion and purification systems via Fe_3O_4@TiO_2 nanoparticles. Energy Conversion and Management 2018; 171: 272-278.

[14] Bahiraei M, Hangi M. Flow and heat transfer characteristics of magnetic nanofluids: A review. Journal of Magnetism and Magnetic Materials 2015; 374:125-138.

[15] Li Y, Hong W, Li H, Yan Z, Wang S, Liu X, Li B, Jiang H, Niu X. Solar absorber with tunable porosity to control the water supply velocity to accelerate water evaporation. Desalination 2021, 511: 115113.

[16] Selimefendigil F, Öztop HF. Corrugated conductive partition effects on MHD free convection of CNT-water nanofluid in a cavity. International Journal of Heat and Mass Transfer 2019; 129: 265-277.

[17] Mei S, Qi C, Liu M, Fan F, Liang L. Effects of paralleled magnetic field on thermo-hydraulic performances of Fe_3O_4-water nanofluids in a circular tube. International Journal of Heat and Mass Transfer 2019; 134: 707-721.

[18] Gupta M, Singh V, Kumar S, Kumar S, Dilbaghi N, Said Z. Up to date review on the synthesis and thermophysical properties of hybrid nanofluids. Journal of Cleaner Production 2018; 190: 169-192.

[19] Wang G, Qi C, Liu M, Li C, Yan Y, Liang L. Effect of corrugation pitch on thermo-hydraulic performance of nanofluids in corrugated tubes of heat exchanger system based on exergy efficiency. Energy Conversion and Management 2019; 186: 51-65.

[20] Sundar LS, Naik MT, Sharma KV, Singh MK, Reddy TCS. Experimental investigation of forced convection heat transfer and friction factor in a tube with Fe_3O_4 magnetic nanofluid. Experimental Thermal and Fluid Science 2012; 37: 65-71.

[21] Wang L, Lin X, Chai L, Peng L, Yu D, Chen H. Cyclic transient behavior of the Joule-Brayton based pumped heat electricity storage : Modeling and analysis. Renewable and Sustainable Energy Reviews 2019; 111: 523-534.

[22] Ren T, Modest M F, Fateev A, Sutton G, Zhao W, Rusu F. Machine learning applied to retrieval of temperature and concentration distributions from infrared emission measurements. Applied Energy 2019; 252: 113448.

[23] Shin D, Banerjee D. Specific heat of nanofluids synthesized by dispersing alumina nanoparticles in alkali salt eutectic. International Journal of Heat and Mass Transfer 2014; 74: 210-4.

[24] Wan X, Feng W, Wang Y, Wang H, Zhang X, Deng C, Yang N. Materials discovery and properties prediction in thermal transport via materials informatics: A mini review. Nano Letter 2019; 19: 3387-3395.

[25] Anirudh K, Dhinakaran S. Effects of Prandtl number on the forced convection heat transfer from a porous square cylinder. International Journal of Heat and Mass Transfer 2018; 126: 1358-1375.

[26] Afrand M. Using a magnetic field to reduce natural convection in a vertical cylindrical annulus. International Journal of Thermal Sciences 2017; 118: 12-23.

[27] Wang X, Yan Y, Meng X, Chen G. A general method to predict the performance of closed pulsating heat pipe by artificial neural network. Applied Thermal Engineering 2019; 157: 113761.

[28] Longo GA, Zilio C, Ceseracciu E, Reggiani M. Application of artificial neural network (ANN) for the prediction

of thermal conductivity of oxide-water nanofluids. Nano Energy 2012; 1: 290-296.

[29] Papari MM, Yousefi F, Moghadasi J, Karimi H, Campo A. Modeling thermal conductivity augmentation of nanofluids using diffusion neural networks. International Journal of Thermal Sciences 2011; 50: 44-52.

[30] Yigit KS, Ertunc HM. Prediction of the air temperature and humidity at the outlet of a cooling coil using neural networks. International Communications in Heat and Mass Transfer 2006; 33: 898-907.

[31] Ariana MA, Vaferi B, Karimi G. Prediction of thermal conductivity of aluminawater-based nanofluids by artificial neural networks. Powder Technology 2015; 278: 1-10.

[32] Al-waeli AHA, Sopian K, Yousif JH, Kazem HA, Boland J, Chaichan MT. Artificial neural network modeling and analysis of photovoltaic/thermal system based on the experimental study. Energy Conversion and Management 2019; 186: 368-379.

[33] Chandrasekar M, Suresh S. A review on the mechanisms of heat transport in nanofluids. Heat Transfer Engineering 2009; 30(14): 1136-1150.

[34] Qi HB, Zhou GZ, Yu FH, Ge W, Li JH. Researches on mixing of granular materials with discrete element method. Progress in Chemistry 2015; 27(1): 113-124.

[35] Mahbubul IM, Saidur R, Amalina MA. Latest developments on the viscosity of nanofluids. International Journal of Heat and Mass Transfer 2012; 55(4): 874-885.

[36] Sajid MU, Ali HM. Recent advances in application of nanofluids in heat transfer devices : A critical review. Renewable and Sustainable Energy Reviews 2019; 103: 556-592.

[37] Hussein AM, Sharma KV, Bakar RA, Kadirgama K. A review of forced convection heat transfer enhancement and hydrodynamic characteristics of a nanofluid. Renewable and Sustainable Energy Reviews 2014; 29: 734-743.

[38] Sekhar YR, Sharma K. Study of viscosity and specific heat capacity characteristics of water-based Al_2O_3 nanofluids at low particle concentrations. Journal of experimental Nanoscience 2015; 10: 86-102.

[39] Gupta M, Singh V, Kumar R, Said Z. A review on thermophysical properties of nanofluids and heat transfer applications. Renewable and Sustainable Energy Reviews 2017; 74: 638-670.

[40] Jia BP, Gao L, Sun J. Self-assembly of magnetite beads along multi-walled carbon nanotubes via a simple hydrothermal process. Carbon 2007; 45: 1476-81.

[41] Afrand M, Toghraie D, Ruhani B. Effects of temperature and nanoparticles concentration on rheological behavior of Fe_3O_4-Ag/EG hybrid nanofluid: an experimental study. Experimental Thermal and Fluid Science 2016; 77: 38-44

[42] Kurt H, Kayfeci M. Prediction of thermal conductivity of ethylene glycol-water solutions by using artificial neural networks. Applied Energy 2009; 86: 2244-2248.

[43] Harandi SS, Karimipour A, Afrand M, D'Orazio A. An experimental study on thermal conductivity of F-MWCNTs–Fe_3O_4/EG hybrid nanofluid: effects of temperature and concentration. International Communications in Heat and Mass Transfer 2016; 76: 171-177.

[44] Shi L, He Y, Huang Y, Jiang B. Recyclable Fe_3O_4@CNT nanoparticles for high-efficiency solar vapor generation. Energy Conversion and Management 2017; 149: 401-408.

[45] Li Q, Xuan Y, Wang J. Experimental investigations on transport properties of magnetic fluids. Experimental Thermal and Fluid Science 2005; 30(2): 109-116.

[46] T.X. Phuoc, M. Massoudi, Experimental observations of the effects of shear rates and particle concentration on the viscosity of Fe_2O_3-deionized water nanofluids. International Journal of Thermal Sciences 2009; 48: 1294-1301.

[47] Abareshi M, Goharshadi EK, Mojtaba S. Fabrication, characterization and measurement of thermal conductivity of Fe_3O_4 nanofluids. Journal of Magnetism and Magnetic Materials 2010; 322: 3895-3901.

[48] Wright B, Thomas D, Hong H, Groven L, Puszynski J, Duke E, Ye X, Jin S. Magnetic field enhanced thermal conductivity in heat transfer nanofluids containing Ni coated single wall carbon nanotubes. Applied Physics Letters 2010; 173116.

[49] Sundar LS, Ramana EV, Singh MK, De Sousa ACM. Viscosity of low volume concentrations of magnetic Fe_3O_4 nanoparticles dispersed in ethylene glycol and water mixture. Chemical Physics Letters 2012; 554: 236-242.

[50] Colla L, Fedele L, M. Scattolini, Bobbo S. Water-based Fe_2O_3 nanofluid characterization: thermal conductivity and viscosity measurements and correlation. Advances in Mechanical Engineering 2012; 674947.

[51] Ghofrani A, Dibaei MH, Sima AH, Shafii MB. Experimental investigation on laminar forced convection heat transfer of ferrofluids under an alternating magnetic field. Experimental Thermal and Fluid Science 2013; 49: 193-200.

[52] Sundar LS, Singh MK, Sousa ACM. Investigation of thermal conductivity and viscosity of Fe_3O_4 nanofluid for heat transfer applications. International communications in heat and mass transfer 2013; 44:7-14.

[53] Yu W, Xie H, Chen L, Li Y. Enhancement of thermal conductivity of kerosene-based Fe_3O_4 nanofluids prepared via phase-transfer method. Colloids and Surfaces A: Physicochemical and Engineering Aspects, 2010, 355(1-3): 109-113.

[54] Sundar LS, Singh MK, Sousa ACM. Enhanced heat transfer and friction factor of MWCNT-Fe_3O_4/water hybrid

nanofluids. International Communications in Heat and Mass Transfer, 2014, 52: 73-83.

[55] Sundar LS, Singh MK, Bidkin I, Sousa ACM. Transfer Experimental investigations in heat transfer and friction factor of magnetic Ni nanofluid flowing in a tube, International Journal of Heat and Mass Transfer 2014; 70: 224-234.

[56] Esfe M H, Saedodin S, Wongwises S, Toghraie D. An experimental study on the effect of diameter on thermal conductivity and dynamic viscosity of Fe/water nanofluids. Journal of Thermal Analysis and Calorimetry 2015; 119(3): 1817-1824.

[57] Mariano A, Pastoriza-Gallego MJ, Lugo L, Mussari L, Piñeiro MM. Co_3O_4 ethylene glycol-based nanofluids: thermal conductivity, viscosity and high pressure density. International Journal of Heat and Mass Transfer 2015; 85: 54-60.

[58] Karimi A, Amin M, Sadatlu A, Saberi B, Shariatmadar H. Experimental investigation on thermal conductivity of water based nickel ferrite nanofluids. Advanced Powder Technology 2015; 26: 1529-1536.

[59] Afrand M, Toghraie D, Sina N. Experimental study on thermal conductivity of water-based Fe_3O_4 nanofluid: development of a new correlation and modeled by artificial neural network. International Communications in Heat and Mass Transfer 2016; 75: 262-269.

[60] Harandi SS, Karimipour A, Afrand M, Akbari M, D'Orazio A. An experimental study on thermal conductivity of F-MWCNTs-Fe_3O_4/EG hybrid nanofluid: effects of temperature and concentration. International Communications in Heat and Mass Transfer 2016; 76: 171-177.

[61] Shahsavar A, Saghafian M, Salimpour M, Shafii, M. Experimental investigation on laminar forced convective heat transfer of ferrofluid loaded with carbon nanotubes under constant and alternating magnetic fields. Experimental Thermal and Fluid Science 2016; 76: 1-11.

[62] Wang L, Wang Y, Yan X, Wang X, Feng B. Investigation on viscosity of Fe_3O_4 nanofluid under magnetic field. International Communications in Heat and Mass Transfer 2016; 72: 23-28.

[63] Kumar N, Sonawane SS. Experimental study of Fe_2O_3/water and Fe_2O_3/ethylene glycol nanofluid heat transfer enhancement in a shell and tube heat exchanger. International Communications in Heat and Mass Transfer 2016; 78: 277-284.

[64] Nurdin I, Idris I, Rafie M. Enhancement of thermal conductivity and kinematic viscosity in magnetically controllable maghemite (γ-Fe_2O_3) nanofluids. Experimental Thermal and Fluid Science 2016; 72: 265-271.

[65] Esfe MH, Hajmohammad MH. Thermal conductivity and viscosity optimization of nanodiamond-Co_3O_4/EG (40:60) aqueous nanofluid using NSGA-II coupled with RSM. Journal of Molecular Liquids 2017; 238: 545-

552.

[66] Amani M, Ama P, Kasaeian A, Mahian O, Pop I. Modeling and optimization of thermal conductivity and viscosity of $MnFe_2O_4$ nanofluid under magnetic field using an ANN. Scientific Reports 2017; 1-13.

[67] Vinod S, Philip J. Experimental evidence for the significant role of initial cluster size and liquid confinement on thermo-physical properties of magnetic nanofluids under applied magnetic field. Journal of Molecular Liquids 2018; 257: 1-11.

[68] Shi L, He Y, Hu Y, Wang X. Thermophysical properties of Fe_3O_4@CNT nanofluid and controllable heat transfer performance under magnetic field. Energy Conversion and Management 2018; 177: 249-257.

[69] Fu R, Liu Z, Chen Y, Yan Y. Experimental investigation of turbulent forced heat transfer of Fe_3O_4 ethylene glycol-Water nanofluid with highly disaggregated particles. Thermal Science and Engineering Progress 2019; 10: 1-9.

[70] Esen H, Inalli M, Sengur A, Esen M. Performance prediction of a groundcoupled heat pump system using artificial neural networks. Expert Systems with Applications 2008; 35:1940-8.

[71] Aydinalp M, Ugursal VI, Fung AS. Modelling of the appliance, lighting and space-cooling energy consumption in the residential sector using neural networks. Applied Energy 2002; 71: 87-110.

[72] Lin C, Wang J, Chen T. Analysis of suspension and heat transfer characteristics of Al_2O_3 nanofluids prepared through ultrasonic vibration. Applied Energy 2011; 88: 4527-4533.

[73] Aladag B, Halelfadl S, Doner N, Maré T, Duret S, Estellé P. Experimental investigations of the viscosity of nanofluids at low temperatures. Applied Energy 2012; 97: 876-880.

[74] Shi D, Cheng JP, Liu F, Zhang XB. Controlling the size and size distribution of magnetite nanoparticles on carbon nanotubes. Journal of Alloys and Compounds 2010; 502: 365-70.

[75] Maxwell JC. A treatise on electricity and magnetism. London: Oxford University Press; 1904.

[76] Hamilton R, Crosser O. Thermal conductivity of heterogeneous two-component systems. Industrial & Engineering Chemistry Fundamentals 1962; 1: 187-91.

[77] Wasp EJ, Kenny JP, Gandhi RL. Solid-liquid flow slurry pipeline transportation: Gulf Publishing Company; 1979.

[78] Yu W, Choi S. The role of interfacial layers in the enhanced thermal conductivity of nanofluids: a renovated Maxwell model. Journal of Nanoparticle Research 2003; 5:167-71.

[79] Jang SP, Choi SU. Role of Brownian motion in the enhanced thermal conductivity of nanofluids. Applied Physics Letters 2004; 84:4316-8.

[80] Koo J, Kleinstreuer C. A new thermal conductivity model for nanofluids. Journal of Nanoparticle Research 2004; 6:577-88.

[81] Chon CH, Kihm KD, Lee SP, Choi SU. Empirical correlation finding the role of temperature and particle size for nanofluid (Al_2O_3) thermal conductivity enhancement. Applied Physics Letters 2005; 87:153107.

[82] Maiga SEB, Palm SJ, Nguyen CT, Roy G, Galanis N. Heat transfer enhancement by using nanofluids in forced convection flows. International Journal of Heat and Fluid Flow 2005; 26:530-46.

[83] Prasher R, Bhattacharya P, Phelan PE. Thermal conductivity of nanoscale colloidal solutions (nanofluids). Physical Review Letters 2005; 94(2): 025901.

[84] Patel HE, Anoop K, Sundararajan T, Das SK. A micro-convection model for thermal conductivity of nanofluids. International Heat Transfer Conference 13: Begel House Inc; 2006.

[85] Timofeeva EV, Routbort JL, Singh D. Particle shape effects on thermophysical properties of alumina nanofluids. Journal of Applied Physics 2009; 106(1): 014304.

[86] Vajjha RS, Das DK. Experimental determination of thermal conductivity of three nanofluids and development of new correlations. International Journal of Heat and Mass Transfer 2009; 52: 4675-4682.

[87] Corcione M. Empirical correlating equations for predicting the effective thermal conductivity and dynamic viscosity of nanofluids. Energy Conversion Management 2011; 52:789-93.

[88] Nkurikiyimfura I, Wang Y, Pan Z. Effect of chain-like magnetite nanoparticle aggregates on thermal conductivity of magnetic nanofluid in magnetic field. Experimental Thermal and Fluid Science 2013; 44: 607-612.

[89] Sharma KV, Sarma PK, Azmi WH, Mamat R, & Kadirgama K. Correlations to predict friction and forced convection heat transfer coefficients of water based nanofluids for turbulent flow in a tube. International Journal of Microscale and Nanoscale Thermal and Fluid Transport Phenomena 2012; 3(4): 283.

[90] Sundar LS, Ramana EV, Singh MK, Sousa AC. Thermal conductivity and viscosity of stabilized ethylene glycol and water mixture Al_2O_3 nanofluids for heat transfer applications: An experimental study. International Communications in Heat and Mass Transfer 2014; 56: 86-95.

[91] Esfe MH, Saedodin S, Wongwises S, Toghraie D. An experimental study on the effect of diameter on thermal conductivity and dynamic viscosity of Fe/water nanofluids. Journal of Thermal Analysis and Calorimetry 2015; 119: 1817-24.

[92] Hassani S, Saidur R, Mekhilef S, Hepbasli A. A new correlation for predicting the thermal conductivity of nanofluids; using dimensional analysis. International Journal of Heat and Mass Transfer, 2015; 90: 121-30.

[93] Okonkwo EC, Wole-Osho I, Almanassra IW, Abdullatif YM, Al-Ansari T. An updated review of nanofluids in various heat transfer devices. Journal of Thermal Analysis and Calorimetry 2020; 1-56.

[94] Sezer N, Atieh MA, Koç M. A comprehensive review on synthesis, stability, thermophysical properties, and characterization of nanofluids. Powder Technology 2019, 344: 404-31.

[95] Pak BC, Cho YI. Hydrodynamic and heat transfer study of dispersed fluids with submicron metallic oxide particles. Experimental Heat Transfer an International Journal 1998; 11:151-70.

[96] Koo J, Kleinstreuer C. Impact analysis of nanoparticle motion mechanisms on the thermal conductivity of nanofluids. International Communications in Heat and Mass Transfer 2005; 32:1111-8.

[97] Nguyen C, Desgranges F, Roy G, Galanis N, Mare T, Boucher S, et al. Temperature and particle-size dependent viscosity data for water-based nanofluids-hysteresis phenomenon. International Journal of Heat and Fluid Flow 2007; 28:1492-506.

[98] Abu-Nada E. Effects of variable viscosity and thermal conductivity of Al_2O_3-water nanofluid on heat transfer enhancement in natural convection. International Journal of Heat and Fluid Flow 2009; 30:679-90.

[99] Masoumi N, Sohrabi N, Behzadmehr A. A new model for calculating the effective viscosity of nanofluids. Journal of Physics D: Applied Physics 2009; 42(5): 055501.

[100] Esfe MH, Saedodin S, Mahmoodi M. Experimental studies on the convective heat transfer performance and thermophysical properties of MgO-water nanofluid under turbulent flow. Experimental Thermal and Fluid Science 2014; 52:68-78.

[101] Ganvir RB, Walke PV, Kriplani VM, Heat transfer characteristics in nanofluid-A review. Renewable and Sustainable Energy Reviews, 2017, 75: 451-460.

[102] Wang L, Wang Y, Yan X, et al. Investigation on viscosity of Fe_3O_4 nanofluid under magnetic field. International Communications in Heat and Mass Transfer, 2016, 72: 23-28.

[103] Vajjha RS, Das DK. Specific heat measurement of three nanofluids and development of new correlations. Journal of Heat Transfer 2009; 131(7): 071601.

[104] Fakoor Pakdaman M, Akhavan-Behabadi MA, Razi P. An experimental investigation on thermo-physical properties and overall performance of MWCNT/heat transfer oil nanofluids flow inside vertical helically coiled tubes. Experimental Thermal and Fluid Science 2012; 40: 103-11.

[105] Ghazvini M, Akhavan-Behabadi M, Rasouli E, Raisee M. Heat transfer properties of nanodiamond-engine oil nanofluids in laminar flow. Heat Transfer Engineering 2012; 33: 525-32.

[106] Sheikholeslami M, Gorji-Bandpy M, and Ganji D. Lattice Boltzmann method for MHD natural convection heat

transfer using nanofluid. Powder Technology 2014; 254: 82-93.

[107] Ding Y, Alias H, Wen D, Williams R, Heat transfer of aqueous suspensions of carbon nanotubes (CNT Nanofluid). International Journal of Heat and Mass Transfer 2006; 49: 240-250.

[108] Zhu HT, Zhang CY, Liu SQ, Tang YM, Yin YS. Effects of nanoparticle clustering and alignment on thermal conductivities of aqueous nanofluids. Applied Physics Letters 2006; 89(2): 023123.

[109] Zhang Q, Zhu M, Zhang Q, Li Y, Wang H. The formation of magnetite nanoparticles on the sidewalls of multi-walled carbon nanotubes. Composites Science and Technology 2009; 69: 633-8.

[110] Fujita T, Jeyadevan B, Yamaguchi K, Nishiyama H. Preparation, viscosity and damping of functional fluids that respond to both magnetic and electric fields. Powder Technology 1999; 101(3): 279-287.

[111] Afrand M, Rostami S, Akbari M, Wongwises S, Esfe MH, Karimipour A. Effect of induced electric field on magneto-natural convection in a vertical cylindrical annulus filled with liquid potassium. International Journal of Heat and Mass Transfer 2015; 90: 418-426.

[112] Oya T, Nomura T, Tsubota M, Okinaka N, Akiyama T. Thermal conductivity enhancement of erythritol as PCM by using graphite and nickel particles. Applied Thermal Engineering 2013; 61(2): 825-828.

[113] Mo S, Chen Y, Jia L, Luo X. Investigation on crystallization of TiO_2-water nanofluids and deionized water. Applied Energy 2012; 93: 65-70.

[113] Gang W, Wang J, Wang S. Performance analysis of hybrid ground source heat pump systems based on ANN predictive control. Applied Energy 2014; 136: 1138-1144.

[114] Rahimikhoob A. Estimating global solar radiation using artificial neural network and air temperature data in a semi-arid environment. Renewable Energy 2010; 35(9): 2131-2135.

[115] Kalogirou SA. Artificial neural networks in the renewable energy systems applications: a review. Renewable and Sustainable Energy Reviews 2001; 5: 373-401.

[116] Kurt H, Atik K, Ozkaymak M, Binark AK. The artificial neural networks approach for evaluation of temperatureand density profiles of salt gradient solar pond. Journal of the Energy Institute 2006; 80(1): 46-51.

[117] Yang IH, Yeo MS, Kim KW. Application of artificial neural network to predict the optimal start time for heating system in building. Energy Conversion and Management 2003; 4: 2791-809.

[118] Ertunc HM, Hosoz M. Artificial neural network analysis of a refrigeration system with an evaporative condenser. Applied Thermal Engineering 2006; 26: 627-35.

[119] Hojjat M, Etemad SG, Bagheri R, Thibault J. Thermal conductivity of non-Newtonian nanofluids: experimental data and modeling using neural network. International Journal of Heat and Mass Transfer 2011; 54: 1017-1023.

[120] Islamoglu Y, Kurt A, Parmaksızoglu C. Performance prediction for nonadiabatic capillary tube suction line heat exchanger: an artificial neural network approach. Energy Conversion and Management 2005; 46: 223-32.

[121] Al-waeli AHA, Kazem HA, Yousif JH, Chaichan MT, Sopian K. Mathematical and neural network modeling for predicting and analyzing of nanofluid-nano PCM photovoltaic thermal systems performance. Renewable Energy 2020; 145: 963-980.

[122] Xu J, Gao B, Kang F. A reconstruction of Maxwell model for effective thermal conductivity of composite materials, Applied Thermal Engineering 2016; 102: 972-979.

[123] Mohanraj M, Jayaraj S, Muraleedharan C. Applications of artificial neural networks for refrigeration, air-conditioning and heat pump systems-a review. Renewable and Sustainable Energy Reviews 2012; 16: 1340-1358.

[124] Behrang MA, Assareh E, Ghanbarzadeh A, Noghrehabadi AR. The potential of different artificial neural network (ANN) techniques in daily global solar radiation modeling based on meteorological data. Solar Energy 2010; 84(8): 1468-1480

[125] Al-waeli A H A, Kazem H A, Yousif J H, Chaichan M T, Sopian K. Mathematical and neural network modeling for predicting and analyzing of nanofluid-nano PCM photovoltaic thermal systems performance. Renewable Energy 2020; 145: 963-980.

[126] Xu J, Gao B, Kang F. A reconstruction of Maxwell model for effective thermal conductivity of composite materials, Applied Thermal Engineering 2016; 102: 972-979.

[127] Mohanraj M, Jayaraj S, Muraleedharan C. Applications of artificial neural networks for refrigeration, air-conditioning and heat pump systems-a review. Renewable and Sustainable Energy Reviews 2012; 16: 1340-1358.

[128] Behrang MA, Assareh E, Ghanbarzadeh A, Noghrehabadi AR. The potential of different artificial neural network (ANN) techniques in daily global solar radiation modeling based on meteorological data. Solar Energy 2010; 84(8): 1468-1480.

[129] Said Z, Assad MEH, Hachicha AA, Bellos E, Ali M, Zeyad D, Yousef BAA, Enhancing the performance of automotive radiators using nanofluids. Renewable and Sustainable Energy Reviews 2019; 112: 183-194.

[130] Puga J B, Bordalo B D, Silva D J, Dias M M, Belo J H. Novel thermal switch based on magnetic nanofluids with remote activation. Nano Energy, 2017, 31: 278-285.

[131] Rodrigues C, Dias M, Martins L, Silva D, Araújo J, Oliveira J, Pereira A, Ventura J. A magnetically-activated thermal switch without moving parts. Energy Conversion and Management, 2019, 197: 111881.

[132] Zhou H, Zhao W, Zhang H, Wang Y, Wu X, Sun Z. Magnetorheological seal: A review. International Journal of Applied Electromagnetics and Mechanics 2020; 62: 763-786.

[133] Zhou H, Chen Y, Zhang Y, Li D. Simulation and experimental study on pressure transfer mechanism in multitooth magnetic fluid seals. Tribology Transactions 2021; 64(1): 31-41.

[134] Zlotnick HM, Clark AT, Gullbrand SE, Carey JL, Cheng XM, Mauck RL. Magneto-driven gradients of diamagnetic objects for engineering complex tissues. Advanced Materials 2020; 32(48): 2005030.

[135] Ma B, Xu C, Chi J, Chen J, Zhao C, Liu H. A versatile approach for direct patterning of liquid metal using magnetic Field. Advanced Functional Materials 2019; 29: 1901370.

[136] Mehrez Z, El Cafsi, A. Forced convection Fe_3O_4/water nanofluid flow through a horizontal channel under the influence of a non-uniform magnetic field. The European Physical Journal Plus 2021; 136(4): 1-22.

[137] Shi L, Hu Y, He Y. Magnetocontrollable convective heat transfer of nanofluid through a straight tube. Applied Thermal Engineering 2019; 162: 114220.

[138] Yang C, Liu Z, Yu M, Bian X. Magnetic nanofluid based on amorphous Fe-Ni-B@OA particles applied in the treatment of oil slick. Soft Materials 2021; 19(2): 159-167.

[139] Guo K, Chang F, Li H. Application of a magnetic field in saturated film boiling of a magnetic nanofluid (MNF) under reduced gravity. Energies 2021; 14(3): 634.

[140] Xia BH, Wang J, Tian Y, Chen Q, Du X, Zhang Y. Ferrofluids for Fabrication of remotely controllable micro-nanomachines by two-photon polymerization. Advanced Materials 2010; 3204-3207.

[141] Tang Y, Jin T, Flesch RC, Gao Y, He M. Effect of nanofluid distribution on therapeutic effect considering transient bio-tissue temperature during magnetic hyperthermia. Journal of Magnetism and Magnetic Materials 2021; 517: 167391.

[142] Ahmed S, Xu H. Forced convection with unsteady pulsating flow of a hybrid nanofluid in a microchannel in the presence of EDL, magnetic and thermal radiation effects. International Communications in Heat and Mass Transfer 2021; 120: 105042.

[143] Abdulkadhim A, Hamzah HK, Ali FH, Yıldız Ç, Abed AM, Abed EM, Arıcı M. Effect of heat generation and heat absorption on natural convection of Cu-water nanofluid in a wavy enclosure under magnetic field. International Communications in Heat and Mass Transfer 2021; 120: 105024.

[144] Akram S, Afzal Q, Aly Emad H. Half-breed effects of thermal and concentration convection of peristaltic pseudoplastic nanofluid in a tapered channel with induced magnetic field. Case Studies in Thermal Engineering 2020; 22:100775.

[145] Katta R, Jayavel P. Heat transfer enhancement in radiative peristaltic propulsion of nanofluid in the presence of induced magnetic field. Numerical Heat Transfer, Part A: Applications 2020; 79(2): 83-110.

[146] Shi L, Hu Y, Bai Y, He Y. Dynamic tuning of magnetic phase change composites for solar-thermal conversion and energy storage. Applied Energy 2020; 263: 114570.

[147] Ijaz Khan M, Qayyum S, Farooq S, Chu Y, Kadry S. Modeling and simulation of micro-rotation and spin gradient viscosity for ferromagnetic hybrid (Manganese Zinc Ferrite, Nickle Zinc Ferrite) nanofluids. Mathematics and Computers in Simulation 2021; 185: 497-509.

[148] Zhang Y, Wu J, He J, Wang K, Yu G. Solutions to obstacles in the commercialization of room-temperature magnetic refrigeration. Renewable & Sustainable Energy Reviews 2021; 143, 110933.

[149] Zhang X, Zhang Y. Experimental study on enhanced heat transfer and flow performance of magnetic nanofluids under alternating magnetic field. International Journal of Thermal Sciences 2021; 164: 106897.

[150] Rajarathinam M, Chamkha AJ. Effect of partial open on natural convection heat transfer of CNT-water nanofluid in a square cavity with magnetic field. The European Physical Journal Plus 2021; 136(1): 52.

[151] Kushawaha D, Yadav S, Singh DK. Magnetic field effect on double-diffusion with magnetic and non-magnetic nanofluids. International Journal of Mechanical Sciences 2021; 191: 106085.

[152] Raki E, Afrand M, Abdollahi, A. Influence of magnetic field on boiling heat transfer coefficient of a magnetic nanofluid consisting of cobalt oxide and deionized water in nucleate regime: An experimental study. International Journal of Heat and Mass Transfer 2021; 165: 120669.

[153] Rawa M, Abu-Hamdeh N, Golmohammadzadeh A, Goldanlou AS. An investigation on effects of blade angle and magnetic field on flow and heat transfer of non-Newtonian nanofluids: A numerical simulation. International Communications in Heat and Mass Transfer 2021; 120: 105074.

[154] Tian M, Rostami S, Aghakhani S, Goldanlou AS, Qi C. Investigation of 2D and 3D configurations of fins and their effects on heat sink efficiency of MHD hybrid nanofluid with slip and non-slip flow. International Journal of Mechanical Sciences 2020; 189: 105975.

[155] Zhang S, Feng D, Shi L, Wang L, Jin Y, Tian L, Li Z, Wang G, Zhao L, Yan Y. A review of phase change heat transfer in shape-stabilized phase change materials (ss-PCMs) based on porous supports for thermal energy storage. Renewable and Sustainable Energy Reviews 2020; 135: 110127.

[156] Shi L, Hu Y, He Y. Magneto-responsive thermal switch for remote-controlled locomotion and heat transfer based on magnetic nanofluid. Nano Energy 2020; 71: 104582.